An Artificial Molecular Shuttle Operates in Lipid Bilayers for Ion Transport

Sujun Chen,[‡,†] Yichuan Wang,[‡,†] Ting Nie,[†] Chunyan Bao,[*,†] Chenxi Wang,[†] Tianyi Xu,[†] Qiuning Lin,[†] Da-Hui Qu,[*,†] Xueqing Gong,[†] Yi Yang,[§] Linyong Zhu,[*,†] and He Tian[†]

[†]*Key Laboratory for Advanced Materials and Joint International Research Laboratory of Precision Chemistry and Molecular Engineering, Feringa Nobel Prize Scientist Joint Research Center, School of Chemistry and Molecular Engineering, East China University of Science & Technology, 130 Meilong Road, Shanghai, 200237, China*

[§]*Optogenetics & Synthetic Biology Interdisciplinary Research Center, State Key Laboratory of Bioreactor Engineering, School of Pharmacy, East China University of Science & Technology, 130 Meilong Road, Shanghai, 200237, China*

1. General materials.

All starting materials were obtained from commercial suppliers and were used without further purification unless otherwise stated. All air- or moisture-sensitive reactions were performed using oven-dried or flame-dried glassware under an inert atmosphere of dry argon. Air- or moisture-sensitive liquids and solutions were transferred via syringe. Tetrahydrofuran (THF) was distilled from sodium benzophenone; dichloromethane was distilled from calcium hydride; triethylamine (TEA) was redistilled and stored over KOH pellets prior to use. Egg yolk phosphatidylcholine (EYPC) was obtained from Avanti Polar lipids as a solution in chloroform (25 $mg \cdot mL^{-1}$). 8-hydroxy-1,3,6-pyrenetrisulfonate (HPTS), 5(6)-carboxyfluorescein (CF), valinomycin and Trixon-100 were obtained from Sigma-

Aldrich and used without further purification.

2. Characterizations.

^{1}H NMR and ^{13}C NMR were measured on a Brüker AV-400 spectrometer. Chemical shifts were reported in parts per million (ppm) downfield from the Me_4Si resonance which was used as the internal standard when recording ^{1}H NMR spectra. 2D-EXSY spectra were recorded on a Brüker AV-600 spectrometer. The ^{23}Na NMR data was acquired on a Brüker AV-500 spectrometer. The electronic spray ionization (ESI) mass spectra were obtained on a LCT Premier XE mass spectrometer. Fluorescence measurements were performed on a Varian Cary Eclipses fluorescence spectrometer equipped with a stirrer and a temperature controller (kept at 25 ^{o}C unless otherwise noted). A Mini-Extruder used for the preparation of large unilamellar vesicles (LUVs) was purchased from Avanti Polar lipids. The size of EYPC vesicles was determined using a Delsa™ Nano Submicron Particle Size and Zeta Potential Particle Analyzer (Beckman Coulter Inc., USA).

3. Synthesis and characterizations of compounds.

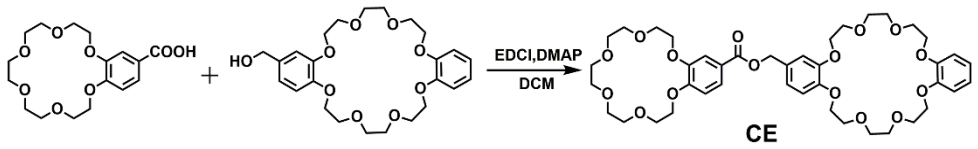

Scheme S1 Synthesis of compound **CE.**

Synthesis of compound CE. To a mixture of 4-carboxy benzo-18-crown-6 (0.435 g, 1.022 mmol) and 4-benzyl alcohol-24-crown-8[1] (0.487 g, 1.224 mmol) in dry DCM (10 mL) was added DMAP (0.124 mg, 1.021 mmol) and EDCI (0.780 mg, 4.070 mmol), and the resulting solution was stirred under argon atmosphere at room temperature for 24 h. Then concentrated hydrochloric acid was added dropwise to the reaction solution

to adjust the pH to 1.0. The obtained solution was diluted with water (50 mL) and extracted with CH_2Cl_2 (3×25 mL). The organic layer was washed with water (3×50 mL), dried over Na_2SO_4 and evaporated in vacuum to give a white solid, which was purified by column chromatography (SiO_2, CH_2Cl_2/MeOH = 150/1) to yield product **CE** as a white solid (0.681 g, 82%).^{1}H NMR (400 MHz, $CDCl_3$) δ: 7.66 (dd, *J* = 8.4, 1.9 Hz, 1H), 7.53 (d, *J* = 1.9 Hz, 1H), 6.98-6.93 (m, 2H), 6.90-6.82 (m, 6H), 5.22 (s, 2H), 4.21-4.13 (m, 12H), 3.97-3.89 (m, 12H), 3.83 (s, 8H), 3.78-3.75 (m, 4H), 3.72-3.70 (m, 4H), 3.68 (s, 4H). ^{13}C NMR (100 MHz, $CDCl_3$) δ: 166.24, 153.04, 148.92, 148.89, 148.84, 148.57, 148.29, 129.22, 124.01, 122.79, 121.70, 121.40, 114.48, 114.30, 113.97, 113.57, 112.05, 71.32, 71.30, 70.95, 70.91, 70.80, 70.72, 70.67, 70.62, 70.56, 69.93, 69.85, 69.48, 69.44, 69.38, 69.33, 69.10, 68.84, 66.53. HRMS (ESI) (m/z): Calcd. for $C_{42}H_{57}O_{16}^+$ $[M+H]^+$: 817.3641, found: 817.3651; Calcd. for $C_{42}H_{56}O_{16}Na^+$ $[M+Na]^+$: 839.3461, found: 839.3459; Calcd. for $C_{42}H_{56}O_{16}K^+$ $[M+K]^+$: 855.3200, found: 855.3212.

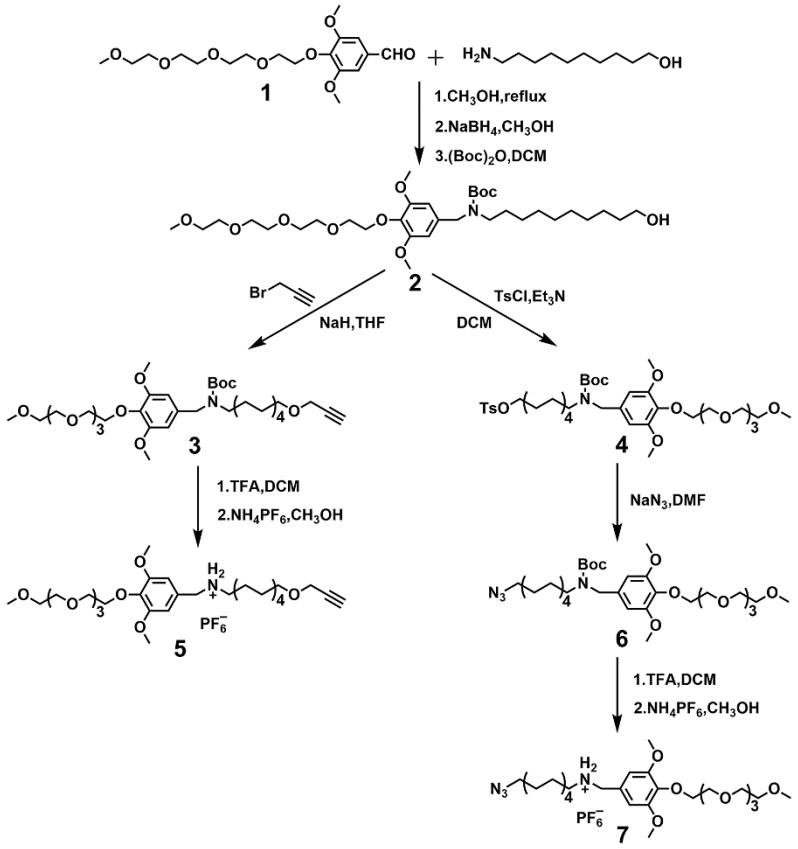

Scheme S2 Synthesis of compound **5** and compound **7.**

Synthesis of compound 2. A mixture of compound **1**[2] (1.012 g, 2.719 mmol) and 10-amino-1-decanol (0.558 g, 3.223 mmol) in dry MeOH (50 mL) was refluxed overnight under argon atmosphere. After being cooled to room temperature, the reaction mixture was added $NaBH_4$ (1.016 g, 26.877 mmol) in portion under ice bath. After the mixture was stirred for 10 h, the solution was poured into water (100 mL) and extracted by CH_2Cl_2 (3 × 50 mL). The organic layer was dried over anhydrous sodium sulfate, and then concentrated to give the amine compound, which was directly dissolved in dry CH_2Cl_2 (10 mL). Boc_2O (5.864 g, 26.874 mmol) was then added and the mixture was stirred for 3 h. The solvent was removed under vacuum, the crude product was purified via column chromatography (SiO_2, CH_2Cl_2/MeOH = 100/1) to give compound **2** (1.258 g, 74%) as a transparent liquid. ^{1}H NMR (400 MHz, $CDCl_3$) δ: 6.43 (s, 2H), 4.34 (s,

2H), 4.10 (t, *J* = 5.1 Hz, 2H), 3.83-3.76 (m, 8H), 3.72 (m, 2H), 3.65 (m, *J* = 12.6, 7.5, 4.9 Hz, 10H), 3.55-3.53 (m, 2H), 3.36 (s, 3H), 3.15 (d, *J* = 30.4 Hz, 2H), 1.76 (s, 4H), 1.56-1.43 (m, 12H), 1.24 (s, 9H). ^{13}C NMR (101 MHz, $CDCl_3$) δ: 153.30, 135.88, 104.50, 103.94, 79.53, 72.16, 71.86, 70.57, 70.54, 70.52, 70.50, 70.42, 70.31, 62.78, 58.96, 56.01, 46.67, 32.71, 29.48, 29.45, 29.38, 29.36, 29.28, 28.43, 26.81, 25.72. HRMS (ESI) (m/z): Calcd. for $C_{33}H_{60}NO_{10}^+$ $[M+H]^+$: 630.4212, found: 630.4212; Calcd. for $C_{33}H_{60}NO_{10}Na^+$ $[M+Na]^+$: 652.4031, found: 652.4041; Calcd. for $C_{33}H_{60}NO_{10}K^+$ $[M+K]^+$: 668.3771, found: 668.3785.

Synthesis of compound 3. To an ice cooled solution of compound **2** (1.303 g, 2.074 mmol) in dry THF (30 mL) was added NaH (0.496 g, 20.672 mmol), and then propargyl bromide (0.738 g, 6.203 mmol). The reaction was kept stirring at room temperature overnight, which was then filtered to remove the solid. After adding saturated sodium chloride solution (50 mL), the solution was extracted with DCM (3×50 mL). Then, the collected organic phase was dried over Na_2SO_4, vacuumed and purified via column chromatography (SiO_2, CH_2Cl_2/MeOH = 150/1) to give compound **3** (1.156 g, 84%) as a transparent liquid. ^{1}H NMR (400 MHz, $CDCl_3$) δ: 6.41 (s, 2H), 4.31 (s, 2H), 4.10-4.08 (m, 4H), 3.82-3.74 (m, 8H), 3.70-3.69 (m, 2H), 3.67-3.60 (m, 8H), 3.53-3.51 (m, *J* = 5.7, 3.6 Hz, 2H), 3.47 (t, *J* = 6.6 Hz, 2H), 3.34 (s, 3H), 3.12 (d, *J* = 29.7 Hz, 2H), 2.39 (t, *J* = 2.4 Hz, 1H), 1.59-1.52 (m, 2H), 1.48-1.40 (m, 10H), 1.31-1.20 (m, 13H). ^{13}C NMR (100 MHz, $CDCl_3$) δ: 153.38, 135.97, 104.55, 104.00, 80.07, 79.51, 74.13, 72.22, 71.95, 70.66, 70.63, 70.60, 70.58, 70.52, 70.37, 70.29, 59.03, 58.02, 56.07, 46.67,

29.55, 29.52, 29.50, 29.41, 29.37, 28.49, 26.90, 26.09. HRMS (ESI) (m/z): Calcd. for $C_{36}H_{61}NO_{10}Na^+$ $[M+Na]^+$: 690.4188, found: 690.4192.

Synthesis of compound 4. Compound **2** (947 mg, 1.498 mmol) and TsCl (573 mg, 3.010 mmol) were dissolved in dry CH_2Cl_2 (10 mL), then Et_3N was added (728 mg, 7.192 mmol) and the mixture was kept stirring at room temperature overnight. After evaporated in vacuum, the crude was further purified by column chromatography (SiO_2, CH_2Cl_2/MeOH = 100/1) to yield product **4** (853 mg, 72%). ^{1}H NMR (400 MHz, $CDCl_3$) δ: 7.78 (d, *J* = 8.3 Hz, 2H), 7.35 (d, *J* = 8.3 Hz, 2H), 6.45 (s, 2H), 4.35 (s, 2H), 4.12 (t, *J* = 5.1 Hz, 2H), 4.01 (t, *J* = 6.5 Hz, 2H), 3.84-3.78 (m, 8H), 3.73-3.72 (m, 2H), 3.71-3.63 (m, 8H), 3.56-3.55 (m, 2H), 3.37 (s, 3H), 3.16 (d, *J* = 28.3 Hz, 2H), 2.45 (s, 3H), 1.67-1.58 (m, 2H), 1.48 (d, *J* = 13.7 Hz, 12H), 1.26 (s, 2H), 1.21 (s, 9H). ^{13}C NMR (100 MHz, $CDCl_3$) δ: 153.31, 144.61, 135.90, 133.15, 129.79, 127.81, 104.48, 103.95, 79.43, 72.15, 71.88, 70.65, 70.59, 70.55, 70.53, 70.44, 70.30, 58.96, 56.00, 46.65, 29.38, 29.25, 28.83, 28.75, 28.42, 26.81, 25.26, 21.58. HRMS (ESI) (m/z): Calcd. for $C_{40}H_{65}NO_{10}SNa^+$ $[M+Na]^+$: 806.4120, found: 806.4131.

Synthesis of compound 5. To a solution of compound **3** (125 mg, 0.208 mmol) in dichloromethane (5 mL) was added TFA (0.5 mL, 6.733 mmol), the obtained mixture was kept stirring for 10 h. Then, a saturated aqueous of NH_4PF_6 (5 mL) was added to the mixture and stirred for another 4 h. The organic layer was separated and evaporated under reduced pressure to get the yellow liquid, which was purified by column chromatography (SiO_2, CH_2Cl_2/MeOH = 75:1) to afford product **5** (135 mg, 92%) as a transparent liquid. ^{1}H NMR (400 MHz, $CDCl_3$) δ: 7.30 (s, 2H), 6.84 (s, 2H), 4.16 (s,

2H), 4.11 (s, 4H), 3.84 (s, 6H), 3.65-3.60 (m, 12H), 3.53-3.47 (m, 4H), 3.19 (s, 3H), 3.11-3.03 (m, 2H), 2.42 (s, 1H), 1.96 (d, *J* = 25.3 Hz, 4H), 1.73 (s, 2H), 1.60-1.51 (m, 2H), 1.25 (d, *J* = 5.6 Hz, 8H). ^{13}C NMR (100 MHz, $CDCl_3$) δ: 153.17, 136.76, 127.10, 107.29, 80.01, 74.21, 72.13, 71.55, 70.66, 70.40, 70.29, 70.20, 58.91, 57.93, 56.11, 52.20, 48.48, 29.42, 29.36, 29.30, 29.11, 26.44, 26.29, 26.00. HRMS (ESI) (m/z): Calcd. for $C_{31}H_{54}NO_8^+$ $[M\text{-}PF_6]^+$: 568.3844, found: 568.3851.

Synthesis of compound 6. In a 25 mL flask, compound **4** (853 mg, 1.092 mmol) and NaN_3 (177 mg, 2.721 mmol) were mixed in dry DMF (10 mL), and the mixture was heated to 80 ºC and kept stirring overnight under the protection of Ar atmosphere. The mixture was poured into 50 mL water and extracted with ethyl acetate (3×25 mL). The organic layer was washed with brine (3×50 mL), dried over Na_2SO_4 and evaporated in vacuum to give a crude product. The purification was performed by column chromatography (SiO_2, CH_2Cl_2/MeOH = 100/1) and pure compound **6** (0.16 g, 47%) was obtained as a transparent liquid. ^{1}H NMR (400 MHz, $CDCl_3$) δ: 6.43 (s, 2H), 4.34 (s, 2H), 4.10 (s, 2H), 3.80 (s, 8H), 3.72-3.64 (m, 1H), 3.54 (s, 2H), 3.37 (s, 3H), 3.25 (t, *J* = 6.8 Hz, 2H), 3.15 (d, *J* = 31.6 Hz, 2H), 1.71 (s, 4H), 1.62-1.55 (m, 2H), 1.47 (d, *J* = 12.0 Hz, 10H), 1.25 (s, 9H). ^{13}C NMR (100 MHz, $CDCl_3$) δ: 153.33, 135.93, 104.52, 103.97, 79.48, 72.18, 71.90, 70.61, 70.58, 70.55, 70.54, 70.47, 70.33, 58.99, 56.03, 51.44, 46.65, 29.67, 29.30, 29.09, 28.80, 28.44, 26.85, 26.67. HRMS (ESI) (m/z): Calcd. for $C_{33}H_{59}N_4O_9^+$ $[M+H]^+$: 655.4277, found: 655.4148; Calcd. for $C_{33}H_{58}N_4O_9Na^+$ $[M+Na]^+$: 677.4096, found: 677.4105; Calcd. for $C_{33}H_{58}N_4O_9K$ $[M+K]^+$: 693.3835, found: 693.3732.

Synthesis of compound 7. The synthesis procedure of compound **7** was similar as that of compound **5**. The crude was purified by column chromatography (SiO_2, CH_2Cl_2 / MeOH = 75:1) to afford product **7** (148 mg, 91%) as a transparent liquid. ^{1}H NMR (400 MHz, $CDCl_3$) δ: 7.11 (s, 2H), 6.77 (s, 2H), 4.15-4.10 (m, 2H), 4.08 (s, 2H), 3.81 (s, 8H), 3.65 (m, 2H), 3.52 (m, 10H), 3.36 (s, 3H), 3.25 (t, *J* = 6.9 Hz, 2H), 1.70 (s, 2H), 1.58 (m, 2H),1.29 (t, *J* = 16.6 Hz, 14H). ^{13}C NMR (100 MHz, $CDCl_3$) δ: 153.20, 127.09, 107.28, 77.35, 77.24, 77.04, 76.72, 71.96, 71.16, 70.08, 69.75, 58.85, 56.14, 51.45, 49.27, 29.29, 29.23, 29.05, 29.02, 28.79, 26.65, 26.36, 26.16. HRMS (ESI) (m/z): Calcd. for $C_{31}H_{54}NO_8^+$ $[M\text{-}PF_6]^+$: 555.3752, found: 555.3755.

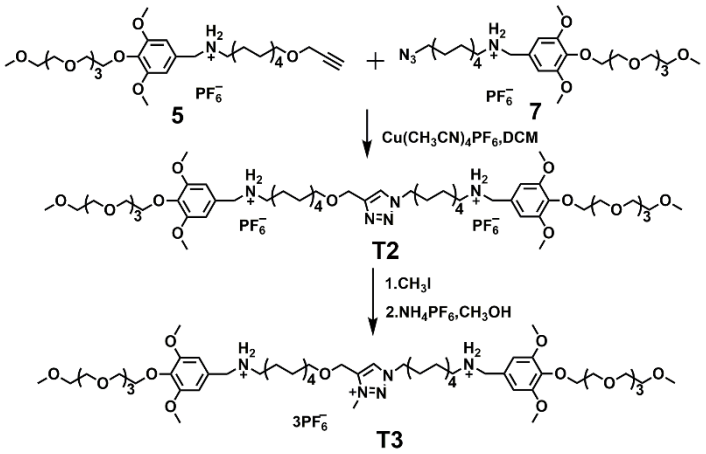

Scheme S3 Synthesis of thread **T2** and **T3**.

Synthesis of thread T2 and T3. In a 25 mL flask, compound **5** (167 mg, 0.234 mmol) and compound **7** (164 mg, 0.234 mmol) were mixed in dry DCM (5 mL), and kept stirring for 2 days under Ar atmosphere. The mixture was poured into 25 mL water and extracted with CH_2Cl_2 (3×25 mL). After removal of the solvent, the residue was purified by column chromatography (SiO_2, CH_2Cl_2 / MeOH = 75 / 1) to give the product **T2** (256 mg, 77%). ^{1}H NMR (400 MHz, CD_3CN) δ: 7.72 (s, 1H), 7.18 (d, *J* = 29.2 Hz, 4H), 6.77 (d, *J* = 5.7 Hz, 4H), 4.47 (s, 2H), 4.33 (t, *J* = 6.9 Hz, 2H), 4.11-4.03 (m, 9H),

3.81 (d, *J* = 2.8 Hz, 13H), 3.73-3.71 (m, 2H), 3.61-3.59 (m, 4H), 3.56-3.43 (m, 25H), 3.30 (t, *J* = 2.0 Hz, 6H), 3.02 (t, *J* = 13.9 Hz, 4H), 1.89-1.80 (m, 2H), 1.65 (s, 4H), 1.53-1.48 (m, 2H), 1.31-1.22 (m, 25H). ^{13}C NMR (100 MHz, CD_3CN, 298K) δ: 153.1, 137.1, 126.4, 107.0, 71.8, 71.2, 70.1, 69.8, 69.8, 69.7, 63.1, 57.7, 55.5, 51.4, 49.5, 47.7, 47.6, 29.3, 29.0, 28.6, 28.5, 28.2, 28.2, 28.1, 27.95, 27.9, 25.6, 25.5, 25.4, 25.3. HRMS (ESI) (m/z): Calcd. for $C_{59}H_{105}N_5O_{15}^{2+}$ $[M\text{-}2PF_6]^{2+}$: 561.8798, found: 561.8786.

T3 was synthesized by dissolving **T2** in CH_3I (5.0 mL) and stirring at 40 °C for 3 d. The reaction mixture was cooled to room temperature, and the excessive CH_3I was evaporated off in vacuum. The residue was dissolved in MeOH (10 mL), followed by the addition of 5.0 mL saturated NH_4PF_6 solution. After the mixture was stirred for 1h, the mixture was extracted with CH_2Cl_2 (3 × 20 mL). The combined organic layer was evaporated, and the residue was purified by column chromatography (SiO_2, CH_2Cl_2 / MeOH = 50 / 1) to give **T3** (250 mg, 88%). ^{1}H NMR (400 MHz, CD_3CN) δ: 8.28 (s, 1H), 7.15 (s, 4H), 6.78 (s, 4H), 4.67 (s, 2H), 4.51 (t, *J* = 7.2 Hz, 2H), 4.16 (s, 3H), 4.09-4.03 (m, 8H), 3.83 (s, 12H), 3.70-3.66 (m, 4H), 3.60 (m, 8H), 3.54 (m, 12H), 3.49 (m, 6H), 3.26 (s, 6H), δ 2.99 (d, *J* = 3.0 Hz, 4H) 2.22-2.21 (m, 6H), 1.59 (m,4H), 1.28 (m, 22H). ^{13}C NMR (100 MHz, CD_3CN) δ: 153.18, 140.70, 136.98, 128.49, 126.23, 117.02, 107.02, 71.77, 71.69, 71.14, 70.97, 69.79, 69.73, 69.63, 60.66, 59.64, 57.68, 55.61, 53.48, 51.30, 47.42, 31.33, 30.27, 29.02, 28.85, 28.74, 28.55, 28.36, 28.29, 28.18, 25.70, 25.38, 25.30, 25.26, 22.08, 13.08. HRMS (ESI) (m/z): Calcd. for $C_{60}H_{108}N_5O_{15}^{3+}PF_6^-$ $[M\text{-}2PF_6]^{2+}$: 641.8736, found: 641.8734.

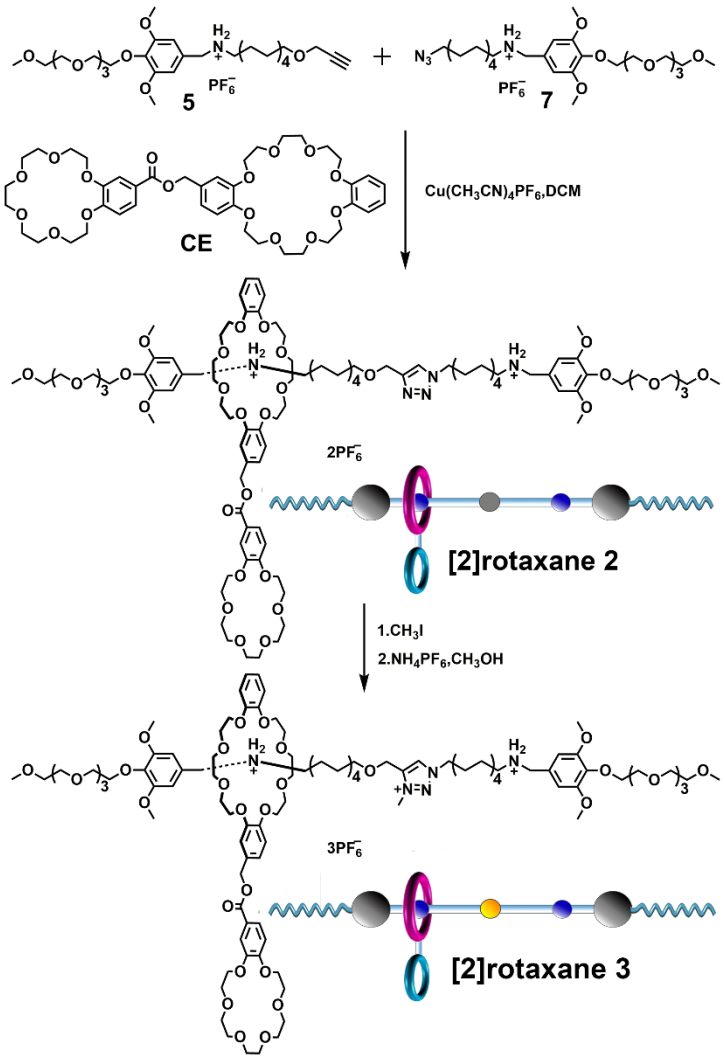

Scheme S4 Synthesis of **[2]rotaxane 2** and **[2]rotaxane 3**.

Synthesis of compound [2]rotaxane 2. A mixture of crown ether **CE** (351 mg, 0.430 mmol) and compound **5** (204 mg, 0.286 mmol) in dry CH_2Cl_2 (8 mL) was stirred at room temperature for 30 minutes. Then compound **7** (200 mg, 0.285 mmol) and $[Cu(CH_3CN)_4]PF_6$ (160 mg, 0.429 mmol) were added to the solution, and the mixture was stirred for 72 h under Ar atmosphere. After removal of the solvent, the residue was purified by column chromatography (SiO_2, CH_2Cl_2 / MeOH = 50 / 1) to give compound **[2]rotaxane 2** (184 mg, 29%). ^{1}H NMR (400 MHz, $CDCl_3$) δ: 7.67-7.58 (m, 2H), 7.46 (s, 1H), 7.15 (s, 2H), 6.98-6.93 (m, 2H), 6.89-6.77 (m, 8H), 6.62 (d, *J* = 1.6 Hz, 2H), 5.20 (d, *J* = 13.7 Hz, 2H), 4.54 (m, 4H), 4.27 (t, *J* = 7.1 Hz, 2H), 4.17-4.07 (m, 12H),

3.97 (d, J = 9.6 Hz, 4H), 3.92-3.74 (m, 18H), 3.62 (m, 48H), 3.52-3.42 (m, 10H), 3.31-3.23 (m, 2H),, 3.11 (s, 2H), 2.93-2.76 (m, 1H), 1.87- 1.45 (m, 6H), 1.40 (m, 2H), 1.24 (m, 16H), 1.02 (m, 8H). ^{13}C NMR (100 MHz, CD_3CN) δ: 165.45, 152.89, 152.74, 151.91, 147.41, 147.05, 144.36, 136.66, 129.26, 127.82, 122.95, 122.78, 121.99, 121.04, 117.03, 112.35, 112.05, 111.90, 111.86, 110.98, 107.65, 106.33, 71.67, 71.60, 71.23, 70.22, 69.81, 69.78, 69.74, 69.62, 69.54, 68.24, 68.15, 67.77, 67.66, 67.42, 65.60, 63.23, 57.56, 55.68, 55.19, 51.92, 50.07, 49.41, 48.40, 45.76, 29.61, 29.56, 29.08, 28.73, 28.54, 28.47, 28.19, 28.14, 28.09, 25.87, 25.74, 25.68, 25.52, 25.10. HRMS (ESI) (m/z): Calcd. for $C_{101}H_{161}N_5O_{31}^{2+}$ $[M\text{-}2PF_6]^{2+}$: 970.5599, found: 970.5604.

Synthesis of compound [2]rotaxane 3. A solution of **[2]rotaxane 2** (81 mg, 0.036 mmol) in CH_3I (5.0 mL) was stirred at 40 ºC for 3 d. The reaction mixture was cooled to room temperature, and the excessive CH_3I was evaporated off in vacuum. The residue was dissolved in MeOH (10 mL), followed by the addition of 5.0 mL saturated NH_4PF_6 solution. After the mixture was stirred overnight, the mixture was extracted with CH_2Cl_2 (3 × 20 mL). The combined organic layer was evaporated, and the residue was purified by column chromatography (SiO_2, CH_2Cl_2 / MeOH = 50 / 1) to give **[2]rotaxane 3** (78 mg, 90%). ^{1}H NMR (400 MHz, $CDCl_3$) δ: 7.66-7.60 (m, 1H), 7.57-7.50 (m, 2H), 7.12 (d, J = 30.9 Hz, 2H), 7.03-6.96 (m, 2H), 6.94-6.81 (m, 8H), 6.67 (s, 2H), 6.42 (s, 2H), 5.22 (s, 2H), 4.62-4.56 (m, 4H), 4.32 (t, J = 7.1 Hz, 4H), 4.26-4.05 (m, 15H), 4.05-4.00 (m, 2H), 3.91 (m, 4H), 3.86-3.74 (m, 18H), 3.72-3.60 (m, 44H), 3.51 (m, 8H), 3.35 (m , 6H), 3.18-3.10 (m, 4H), 2.83-2.74 (m, 2H), 1.90-1.81 (m, 4H), 1.61-1.46 (m, 4H), 1.33-1.17 (m, 16H), 0.98 (m, 8H). ^{13}C NMR (100 MHz, CD_3CN) δ:

165.56, 153.03, 152.80, 152.03, 147.52, 147.12, 144.66, 135.54, 129.47, 126.21, 122.92, 122.70, 122.01, 121.10, 121.06, 112.08, 112.00, 111.02, 108.44, 106.33, 104.14, 78.59, 71.66, 71.28, 70.67, 70.23, 69.86, 69.76, 69.67, 68.20, 67.70, 67.47, 63.27, 57.57, 55.32, 55.20, 53.45, 51.95, 49.43, 47.91, 37.43, 31.37, 29.26, 29.11, 29.01, 28.80, 28.72, 28.64, 28.45, 28.36, 28.17, 27.92, 27.34, 26.15, 25.96, 25.74, 25.57, 23.36, 22.98, 18.85, 13.08. HRMS (ESI) (m/z): Calcd. for $C_{102}H_{164}N_5O_{31}^{3+}$ $[M\text{-}3PF_6]^{3+}$: 652.0476, found: 652.0453.

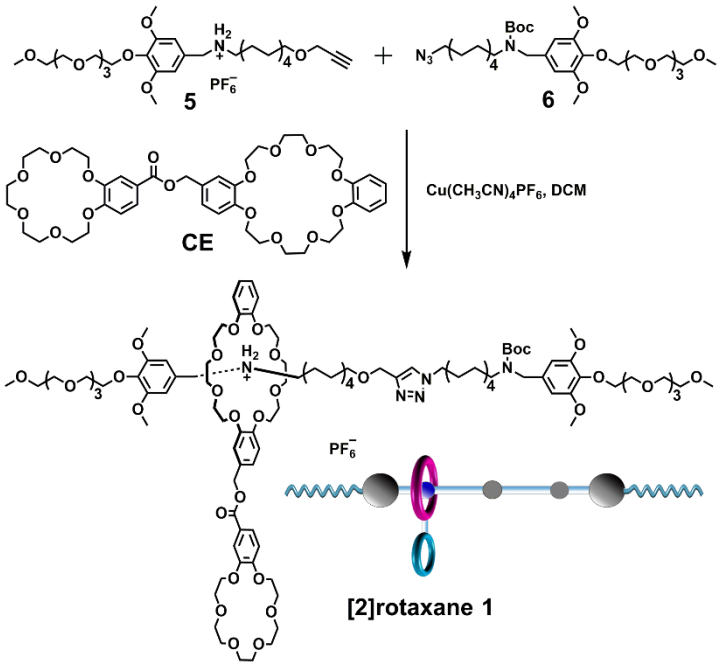

Scheme S5 Synthesis of **[2]rotaxane 1**.

Synthesis of [2]rotaxane 1. The procedure was similar as that for **[2]rotaxane 3**, but using compound **5**, **6** and **CE** as the original compounds. The crude was purified by column chromatography (SiO_2, CH_2Cl_2 / MeOH = 50 / 1) to give compound **[2]rotaxane 1** (236 mg, 49%). ^{1}H NMR (400 MHz, $CDCl_3$) δ: 7.65-7.57 (m, 1H), 7.56-7.47 (m, 2H), 7.12 (s, 2H), 7.02-6.93 (m, 2H), 6.92-6.79 (m, 6H), 6.64 (s, 2H), 6.40 (s, 2H), 5.19 (s, 2H), 4.57 (s, 4H), 4.32-4.27 (m, 4H), 4.24-4.10 (m, 12H), 4.09-4.05 (m,

3H), 4.02-3.98 (m, 2H), 3.91-3.81 (m, 12H), 3.76 (m, 12H), 3.73 (m, 6H), 3.70-3.65 (m, 8H), 3.64-3.60 (m, 18H), 3.59-3.56 (m, 6H), 3.52-3.42 (m, 10H), 3.33 (m, 6H), 3.11 (m, 6H), 1.84 (t, 2H), 1.55-1.50 (m, 2H), 1.46-1.33 (m, 16H), 1.28-1.17 (m, 17H), 0.94 (m, 4H). ^{13}C NMR (100 MHz, $CDCl_3$) δ: 166.14, 161.93, 153.34, 152.72, 148.16, 147.98, 147.86, 147.47, 147.42, 147.33, 140.26, 137.45, 136.33, 135.86, 131.62, 130.03, 128.23, 128.13, 127.89, 124.06, 122.98, 122.60, 122.23, 121.99, 115.78, 113.88, 113.74, 112.67, 111.93, 111.78, 110.41, 106.85, 79.52, 77.39, 77.07, 76.75, 72.70, 72.31, 71.89, 70.77, 70.52, 70.47, 70.33, 70.12, 69.05, 68.25, 67.26, 66.03, 64.19, 59.01, 58.77, 56.06, 52.48, 50.34, 46.69, 42.54, 30.32, 29.69, 29.61, 29.48, 29.32, 29.27, 29.09, 28.99, 28.82, 28.47, 26.86, 26.48, 26.32, 26.04, 14.13, 1.01. HRMS (ESI) (m/z): Calcd. for $C_{106}H_{168}N_5O_{33}^+$ $[M\text{-}PF_6]^+$: 2040.1650, found: 2040.1396.

4. The Molecular dynamic (MD) simulation of T3 in lipid bilayers.

Molecular dynamics (MD) calculations were performed by using the General Utility Lattice Program (GULP) with DREIDING force-field. The model of the lipid bilayer was constructed involving 48 strings of egg yolk phosphatidylcholine (EYPC) molecules and 1344 water molecules, which maintains the radio of the number of water molecules to the number of lipid molecules to be ~28:1. Therein, the structure of one single EYPC molecule was obtained by a molecular dynamics (MD) simulation starting at the temperature of 0 K (10 ps), which was then increased slowly to 300 K (15 ps) and kept for 475 ps. Then, a relatively stable configuration of the EYPC molecule was chosen for the following calculations.

To reduce the computational cost, we chose the thread T3 to demonstrate a stable

membrane-span structure of **T3** in lipid bilayers. After constructing the lipid bilayer, we embedded **T3** in it.

The MD simulation of the complete system was conducted for 150 ps at the constant temperature of 300 K. The time step of the simulation is 0.05 fs. The temperature was kept constant at 300 K, yielding a NVT canonical ensemble. To learn if the T3 can span the lipid bilayer stably, we calculated the system in which the T3 was embedded in the lipid bilayer with surrounding water. As shown in Figure S1, after 27 ps, the temperature was slowly increased to 300 K and kept constant for 10 ps, the system appeared to be rather stable and the T3 was still staying in the lipid bilayer. These results then give strong evidence that the T3 can steadily span the lipid bilayer at 300 K.

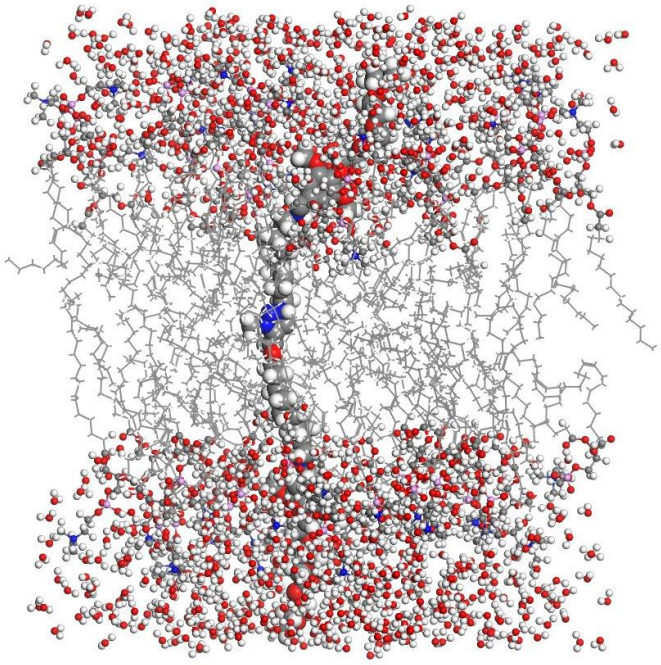

Figure S1 Calculated **T3**-lipid/water system in equilibrium of the molecular dynamics simulation. Water and the hydrophilic part of the lipid bilayer are shown in ball and stick models, the hydrophobic part of the lipid bilayer is shown in line model, **T3** is shown in CPK model. The white, red, grey, blue and pink balls represent hydrogen, oxygen, carbon, nitrogen and phosphorus, respectively.

5. Investigation of shuttling dynamics of [2]rotaxane 3 by 2D-EXSY NMR spectra.[4]

Based on the slow exchange shuttling, the shuttling rate of **[2]rotaxane 3** was estimated by 2D-EXSY consisting of series of 2D-NOESY experiments with different values of mixing time (τ_m, 0.01, 0.1, 0.3 and 0.5 s). In our study, $CDCl_3/CD_3CN$ (1:1, V/V) was selected as the solvent and H_a (6.62 ppm) and $H_{a'}$ (6.78 ppm) were chosen as the peaks A and B. Exchange rates *k* can be obtained by using the equations S1-S2 shown below, where I_{AA} and I_{BB} are the diagonal peak intensities and I_{AB} and I_{BA} are the cross-peak intensities.

$$r = \frac{I_{[AA]}+I_{[BB]}}{I_{[AB]}+I_{[BA]}} \quad \text{Equation S1}$$

$$k = \frac{1}{\tau_m}\ln\frac{r+1}{r-1} \quad \text{Equation S2}$$

k is the sum of forward (k_1) and backward (k_{-1}) (Equation S3). Because **[2]rotaxane 3** is asymmetric, it means here $k_1 \neq k_{-1}$.

$$k = k_1 + k_{-1} \quad \text{Equation S3}$$

To give the value k_1 and k_{-1} respectively, a Windows software EXSYCalc program was used. The final exchange rates were the average values from the calculated rates in different mixing time. According to the **Table S1**, it works out the rate k_1=0.034 Hz, k_{-1}=0.048 Hz, and k=0.082 Hz, respectively.

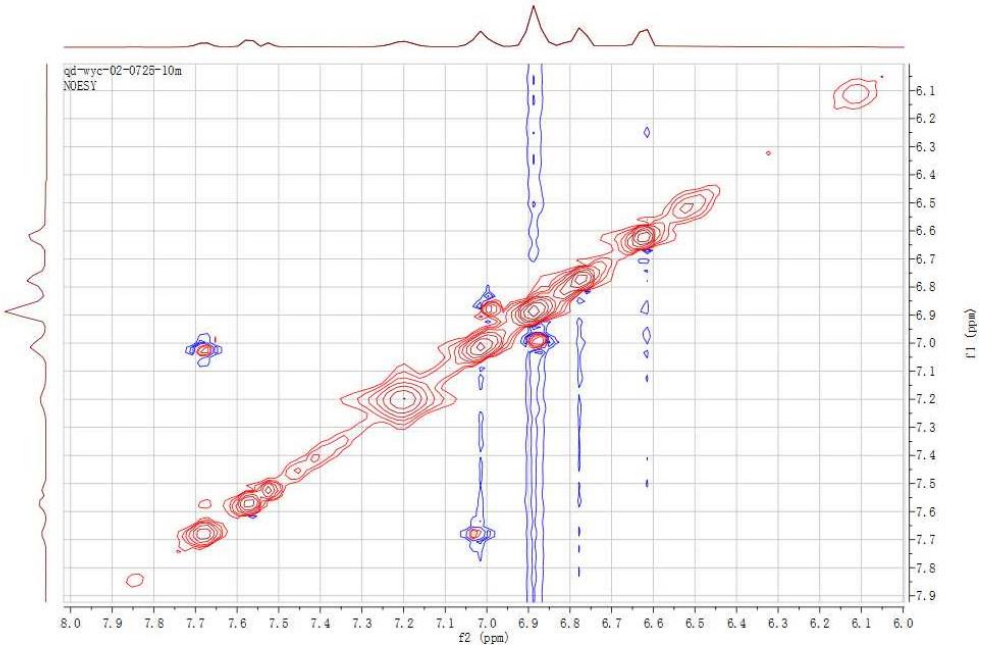

Figure S2 2D EXSY NMR spectrum (600 MHz, 298 K, τ_m= 10 ms) of **[2]rotaxane 3** at 20 mM in CD_3CN / $CDCl_3$ (1:1, v / v).

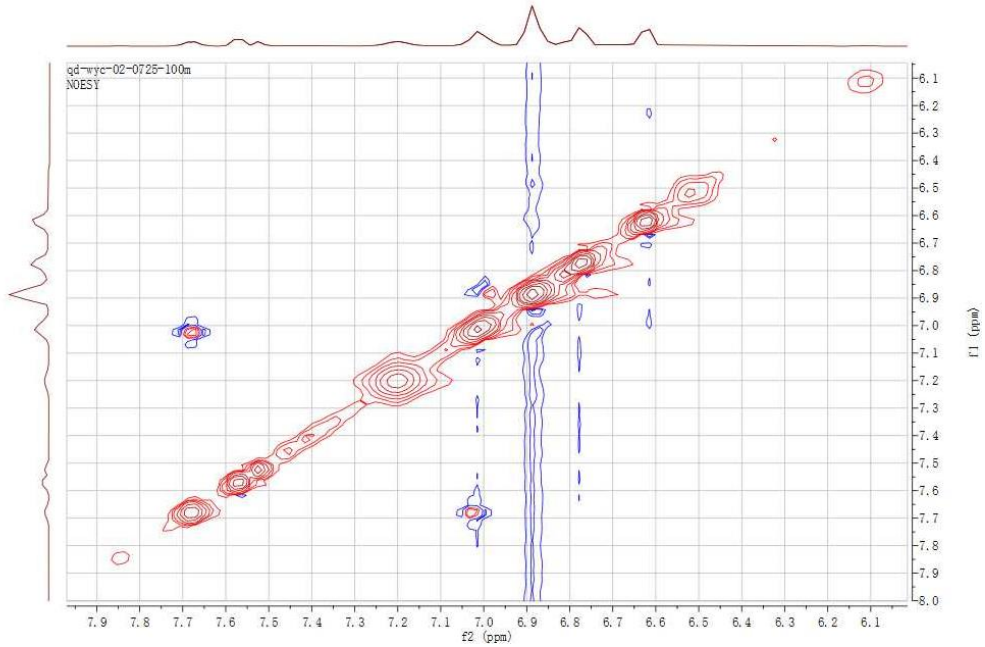

Figure S3 2D EXSY NMR spectrum (600 MHz, 298 K, τ_m = 100 ms) of **[2]rotaxane 3** at 20 mM in CD_3CN / $CDCl_3$ 1:1 (v / v).

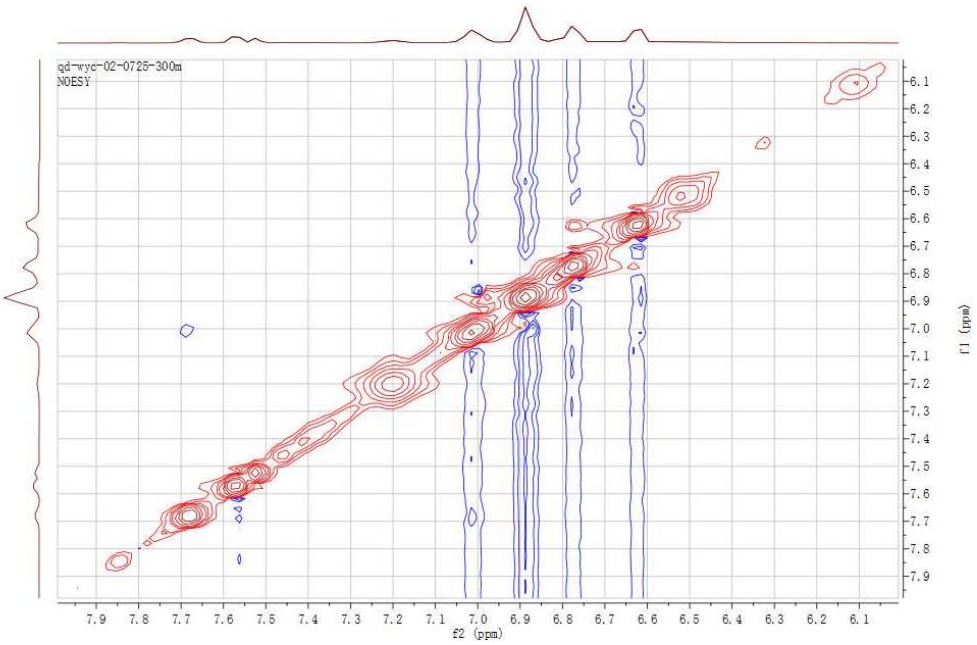

Figure S4 2D EXSY NMR spectrum (600 MHz, 298 K, τ_m = 300 ms) of **[2]rotaxane 3** at 20 mM in CD_3CN / $CDCl_3$ 1:1 (v / v).

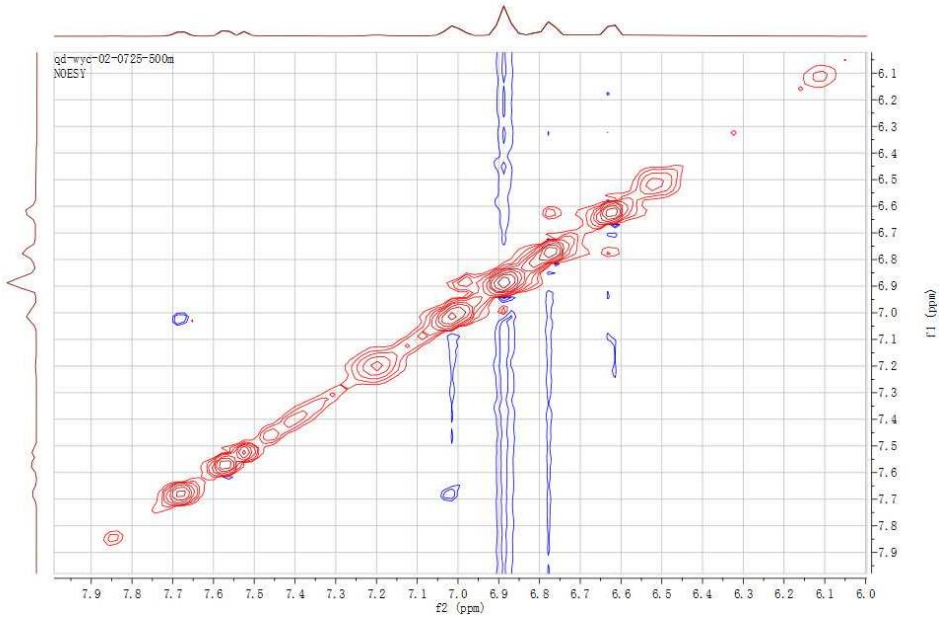

Figure S5 2D EXSY NMR spectrum (600 MHz, 298 K, τ_m = 500 ms) of **[2]rotaxane 3** at 20 mM in CD_3CN / $CDCl_3$ 1:1 (v / v).

Table S1. The integrations of diagonal peaks [AA], [BB] and cross-peaks [AB], [BA] under different τ_m and the exchange rates of forward and reverse shuttling motions calculated by EXSYCalc program.

τ_m / ms	$I_{[AA]}$	$I_{[AB]}$	$I_{[BB]}$	$I_{[BA]}$	k_1 / Hz	k_{-1} / Hz	k / Hz
0	1	0	0.93	0	/	/	/
100	1	0.003	0.902	0.005	0.033	0.051	0.082

300	1	0.010	0.846	0.014	0.037	0.049	0.087
500	1	0.015	0.790	0.019	0.033	0.044	0.076

6. Ion transporting activity studies across LUVs⊃HPTS assay.

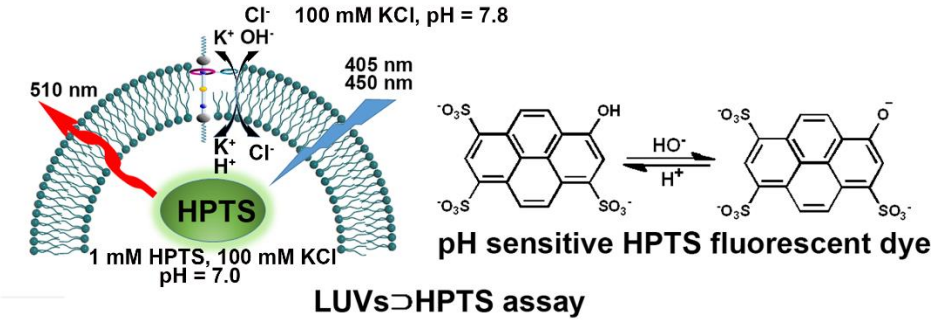

Figure S6 Schematic presentation of LUVs⊃HPTS fluorescence assay for ion transport.

6.1 Preparation of EYPC vesicles enwrapped with HPTS (LUVs⊃HPTS).

A solution of 400 µL egg yolk phosphatidylcholine (EYPC, 25 mg / mL, 10 mg) in deacidified chloroform was mixed with 100 µL of cholesterol (10 mg / mL, 1 mg) in deacidified chloroform. The solvents were evaporated by a slow stream of nitrogen, followed by drying under vacuum for 12 hours. The lipid membrane was hydrated by overtaxing with 500 µL buffer (1 mM HPTS, 10 mM HEPES, 100 mM KCl, pH = 7.0). Then, the suspension was subjected to seven freeze–thaw cycles and allowed to age for 30 min at room temperature before extruding 25 times through a 100 nm polycarbonate membrane. The excess HPTS was separated from the vesicles by size exclusion column chromatography (SephadexG-25) using 100 mM KCl, 10 mM HEPES buffer (pH = 7.0) as eluent. The vesicles were further diluted to reach a total lipid concentration of 1 mM, assuming 100% retention of lipid during the gel filtration process.

6.2 Ion transport activity.

In a typical experiment, 2900 µL of HEPES buffer (10 mM HEPES, 100 mM KCl,

pH = 7.0) was transferred to a quartz cuvette followed by addition of 100 μL of LUVs⊃HPTS (1 mM). The cuvette was placed in the fluorescence instrument with slow stirring condition by a magnetic stirrer equipped in the instrument (at t = 0 s). The time-dependent change in fluorescence intensity (λ_{em} = 510 nm) was monitored at two excitation wavelengths simultaneously ($I_{t,450}$: λ_{ex} = 450 nm, $I_{t,405}$: λ_{ex} = 405 nm), during the addition of base (30 μL, 0.5 M KOH, ΔpH = 0.8) at t = 50 s, transporter (10 μL stock solution in DMSO, 0-50 μM final concentration) at t = 100 s, and 60 μL of 5% Triton X-100 aqueous solution at t = 400 s. All the temperature was kept at 25 °C by a stirrer and a temperature controller. Time courses of fluorescence intensity I_t were obtained by first, ratiometric analysis ($R = I_{t,450} / I_{t,405}$) and second, normalization according to equation Equation S4,

$$I_F = (R - R_{100})/(R_\infty - R_{100}) \qquad \text{Equation S4}$$

where R_{100} is R before addition of transporter and R_∞ is R after addition of Triton X-100. The solvent DMSO (10 μL) was also monitored as the fluorescence background, then, $I = I_F - I_{DMSO}$ was used for data analysis. I at t = 400 s just before addition of Triton X-100 was defined as transmembrane activity Y.

For clarity, the data before the addition of transporter was deleted and time (X-axis) was changed to start from the point of transporter addition (i.e. t = 100 s was normalized to t = 0 s) to the end point of experiment (i.e. t = 400 s was normalized to t = 300 s). The detailed data processing was illustrated in Figure S7.

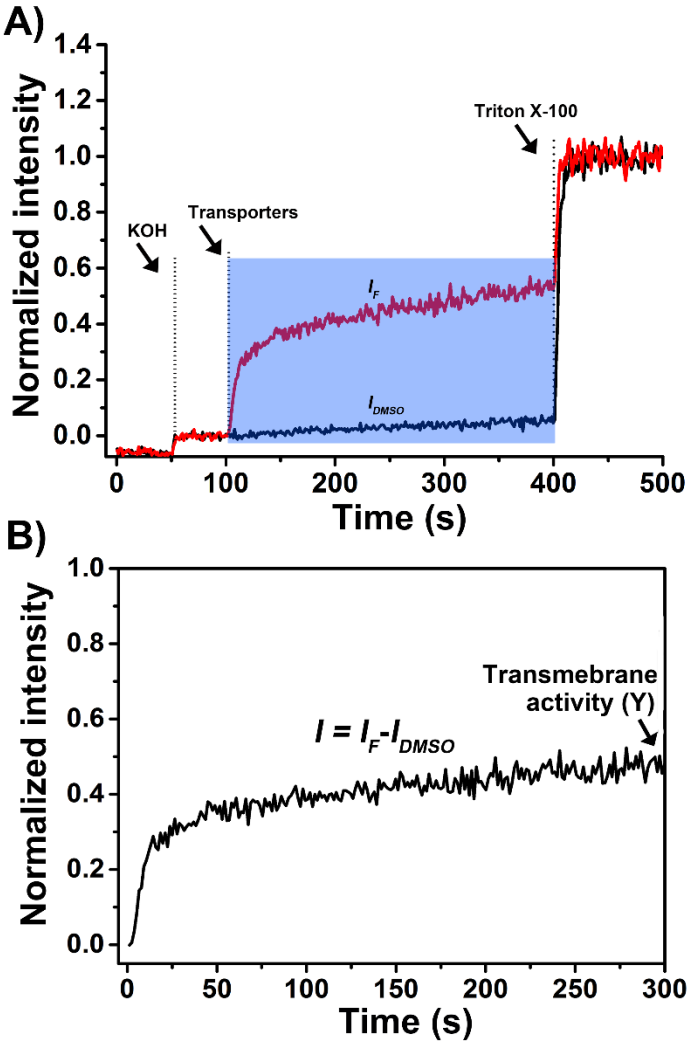

Figure S7 A) Illustration of ion transport kinetics using LUVs⊃HPTS vesicles. B) Final data analysis from the blue window of A). **[2]rotaxane 3** at 1.0 μM (3.0 mol%, relative to lipid) was presented as the example.

The effective concentration EC_{50} (the final concentration of transporter required to obtain 50% activity) was determined from the dosage-transmembrane activity curve fitted by Origin Logistic regression. Figure S8 showed the example of **[2]rotaxane 3**. The EC_{50} values were also presented as transporter to lipid molar ratios.

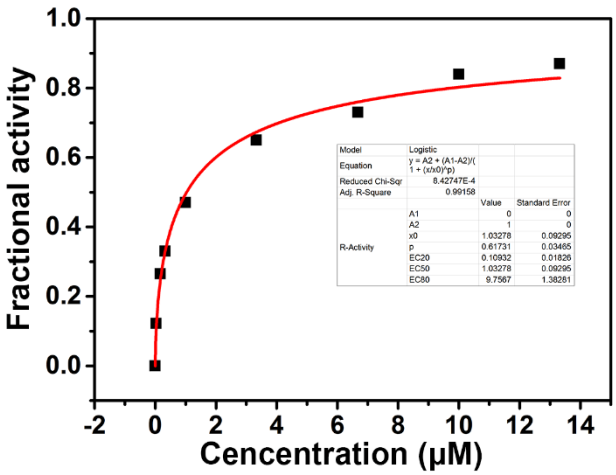

Figure S8 The representative dosage-response curves of **[2]rotaxane 3** in LUVs⊃HPTS assay, which was fitted by Logistic regression to obtain the EC_{50} value of 1.0 μM (3.0 mol%, relative to lipids). The final concentrations of added rotaxane are 0, 0.03, 0.17, 0.33, 1.00, 3.33, 6.67, 10.00, 13.32 μM, respectively.

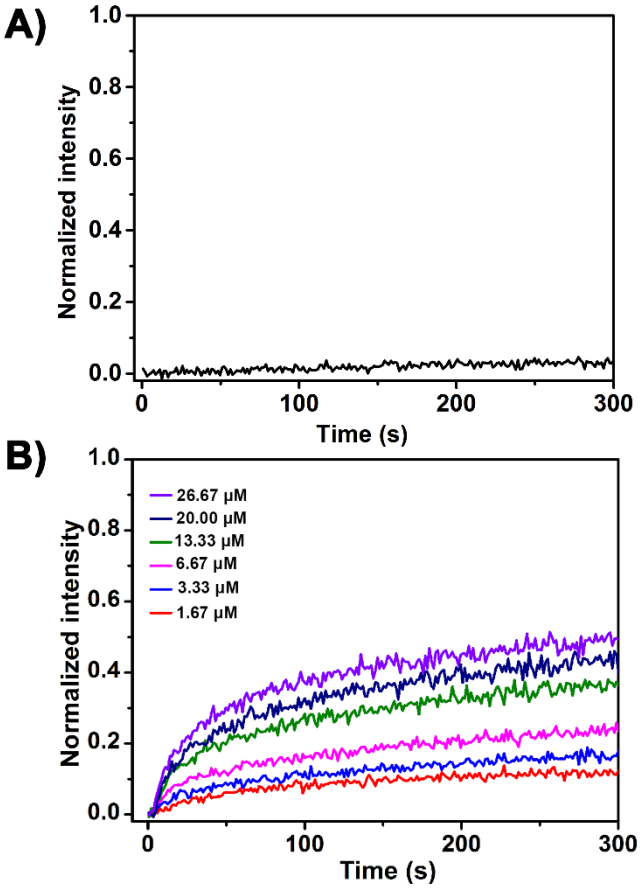

Figure S9 A) The fluorescent evolution of the control experiment (addition with 10 μL DMSO). B) Concentration-dependent enhancement of ion transport activity of thread **T3** with a EC_{50} value of 26.9 μM (81.0 mol%, relative to lipid).

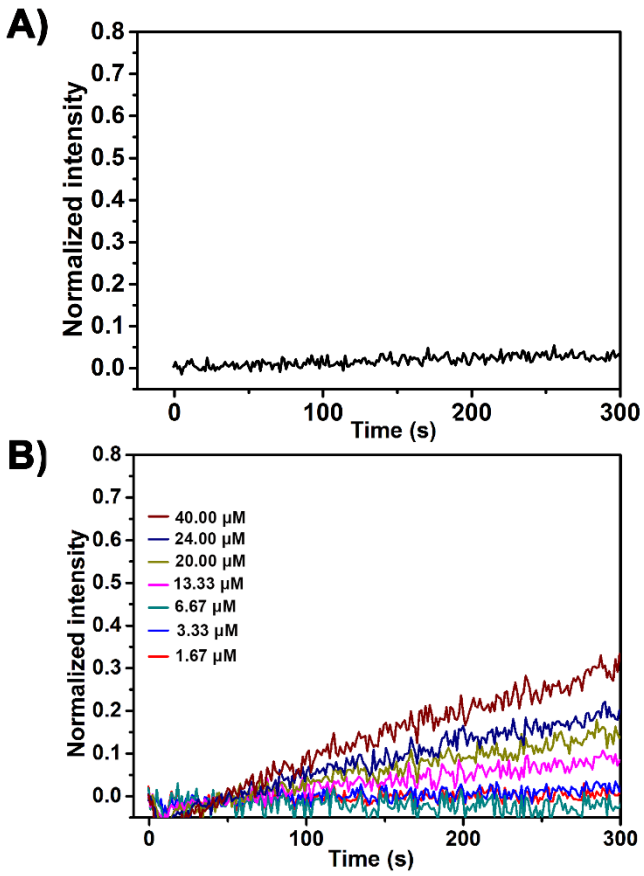

Figure S10 A) The fluorescent evolution of the control experiment (addition with 10 μL DMSO). B) Concentration-dependent enhancement of ion transport activity of **CE**. The EC_{50} value was not determined.

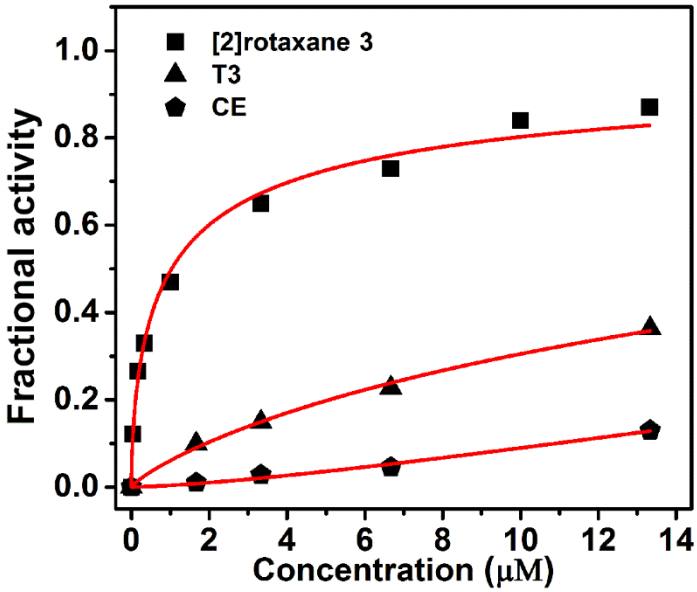

Figure S11 The comparison of transmembrane activities (t = 300 s) among **[2]rotaxane 3**, **thread T3** and wheel **CE** at different concentrations. The red lines were the fitted curves from Logistic regression equation.

6.3 Ion transport rates.

The normalized fluorescence data (*I*) was interactively fitted by a first-order exponential decay equation (equation S5), in which the observed first-order rate constants k_{obs} were obtained.

$$y = y_0(1 - e^{-kt}) \qquad \text{Equation S5}$$

The dependence of the observed rate (k_{obs}) on the concentration of transporters can be used to determine the aggregation state of the channel, or the number of monomers that form the active structure [equation S6].

$$k_{obs} \propto [monomer]^n \qquad \text{Equation S6}$$

If the k_{obs} presented in an linear increase with concentrations, it was indicative of monomolecular active structure for ion transport. To avoid the adverse effects of compounds precipitation, the transport rates k_{obs} were calculated from the data in low concentrations.

For all ion transport experiments, the HPTS assays were repeated for three times and the error bars were less than 5%.

7. 5(6)-carboxyfluorescein (CF) leakage experiment.

The procedure for preparing CF encapsulated LUVs were similar as the LUVs⊃HPTS. The detailed process was described as follows: A solution of 400 μL egg yolk phosphatidylcholine (EYPC, 25 mg / mL, 10 mg) in deacidified chloroform was mixed with 100 μL of cholesterol (10 mg / mL, 1 mg) in deacidified chloroform. The solvents were evaporated by a slow stream of nitrogen, followed by drying under vacuum for 12 hours. The lipid membrane was then hydrated by overtaxing with 500 μL buffer (50 mM CF, 10 mM HEPES, 10 mM KCl, pH = 7.0). Then, the suspension

was subjected to seven freeze–thaw cycles and allowed to age for 30 min at room temperature before extruding 25 times through a 220 nm polycarbonate membrane. The resulted suspension was purified by Sephadex G-50 to remove the extravesicular dye using the same buffer without CF as elute. The obtained vesicles were kept under 4 °C and used within 24 hours. The experimentation and data processing were same as the HPTS assay (section 6.2).

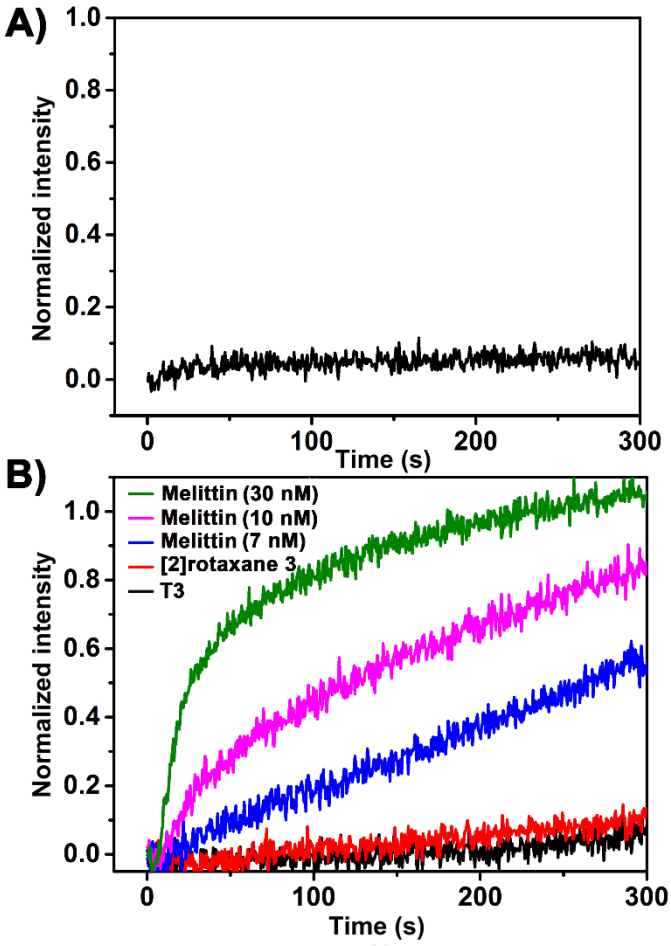

Figure S12 A) The control experiment (addition with 10 μL DMSO) for CF leakage assay. B) CF leakage caused by **[2]rotaxane 3** (1.67 μM, 5.0 mol% relative to lipid), **T3** (6.67 μM, 20.0 mol% relative to lipid) and melittin at different concentrations.

8. The LUVs⊃HPTS with pre-incorporated rotaxane.

A solution of 400 μL egg yolk phosphatidylcholine (EYPC, 25 mg/mL, 10 mg) in deacidified chloroform was mixed with 100 μL of cholesterol (10 mg/mL, 1 mg) and

[2]rotaxane 3 (10 mg / mL, 1 mg, 4 mol% relative to lipid) in deacidified chloroform. The chloroform was removed using a rotary evaporater followed by evacuation on a high vacuum pump line for 12 h. A aqueous solution (0.5 mL, 1 mM HPTS, 10 mM HEPES, 100 mM KCl, pH = 7.0) was added to the lipid film, and vesicle dispersion was obtained by vortexing the flask at room temperature, followed by seven freeze-thaw cycles. The final unilammellar dispersion was extruded 25 times through a 100 nm polycarbonate membrane. The excess HPTS was separated from the vesicles by size exclusion column chromatography (SephadexG-25) using 100 mM KCl, 10 mM HEPES buffer (pH = 7.0) as eluent. The vesicles were further diluted to reach a total lipid concentration of 1 mM, assuming 100% retention of lipid during the gel filtration process. The experimentation and data processing were same as the general HPTS assay (section 6.2).

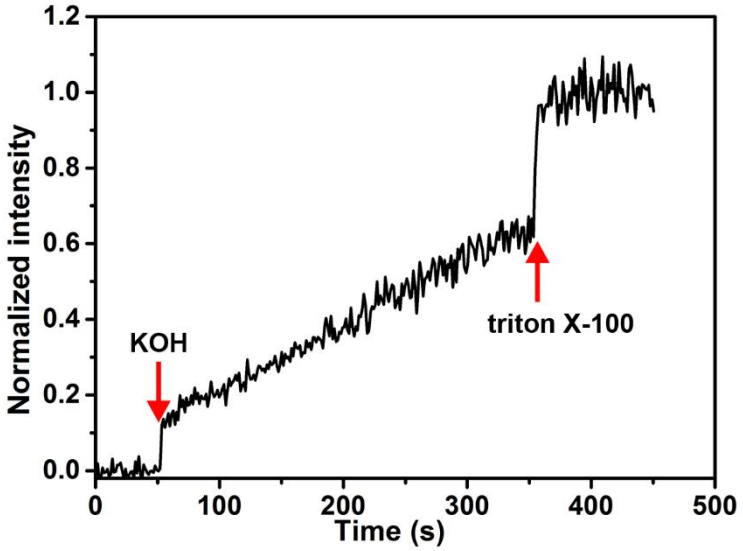

Figure S13 The LUVs⊃HPTS assay for ion transport of pre-incorporated **[2]rotaxane 3** (4.0 mol%, relative to lipid).

9. Patch-clamp measurements on planar lipid bilayer membrane.

DPhPC lipids at 50 mg / mL in chloroform were dried under a stream of nitrogen

and under vacuum each for 4 h, and then dispersed in decane with concentration at 20 mg / mL. The obtained solution was used to precoat a 200 μm hole of a polystyrene cup held by a chamber upon which a planar lipid bilayer membrane was formed. The cup (cis, ground) and chamber (trans) was filled with 1mL 1M KCl solution. Formation of membrane was monitored by measuring membrane capacitance. The transporter in DMSO (0.5 mM) 5 μL was added to the *cis* side of the chamber (final concentration 2.5 μM) and the solution was stirred for 2 minutes. A holding potential of +100 mV was applied and the channel responses were recorded. Ag / AgCl electrodes were used to impose voltages and record currents across the membrane. The patch clamp workstation (Warner Instruments) was used for all experiments. The currents were measured by a Warner BC-535 bilayer clamp amplifier and collected using the Digidata 1550A data acquisition system. All data was filtered at 1 kHz with 8-pole Bessel filter.

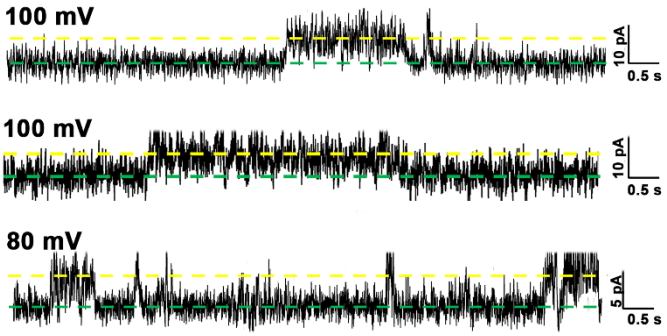

Figure S14 The recorded current profiles of **[2]rotaxane 3** (2.5 μM) from a single channel at different holding potentials in a symmetrical 1 M KCl solution.

10. Ion selectivity studies across LUVs⊃HPTS.

10.1 Preparation of LUVs⊃HPTS Vesicles.

Vesicles were prepared in the same way as stated above (in section 6.2).

10.2 Cation selectivity.

In a typical experiment, 2900 μL of HEPES buffer (10 mM HEPES, 100 mM MCl, pH = 7.0, where, M^+ =Li^+, Na^+, K^+, Rb^+ and Cs^+) was transferred to a quartz cuvette followed by addition of 100 μL of LUVs ⊃HPTS (1mM). The cuvette was placed in the fluorescence instrument with slow stirring condition by a magnetic stirrer equipped in the instrument (at t = 0 s). The time-dependent change in fluorescence intensity (λ_{em} = 510 nm) was monitored at two excitation wavelengths simultaneously ($I_{t,\,450}$: λ_{ex} = 450 nm, $I_{t,\,405}$: λ_{ex} = 405 nm), during the addition of base (30 μL, 0.5 M MOH, M^+ =Li^+, Na^+, K^+, Rb^+ and Cs^+) at t = 50 s, transporter (10 μL stock solution in DMSO) at t = 100 s, and 60 μL of 5% Triton X-100 aqueous solution at t = 400 s. The data analysis and comparison was in the same way as stated above (in section 6.2).

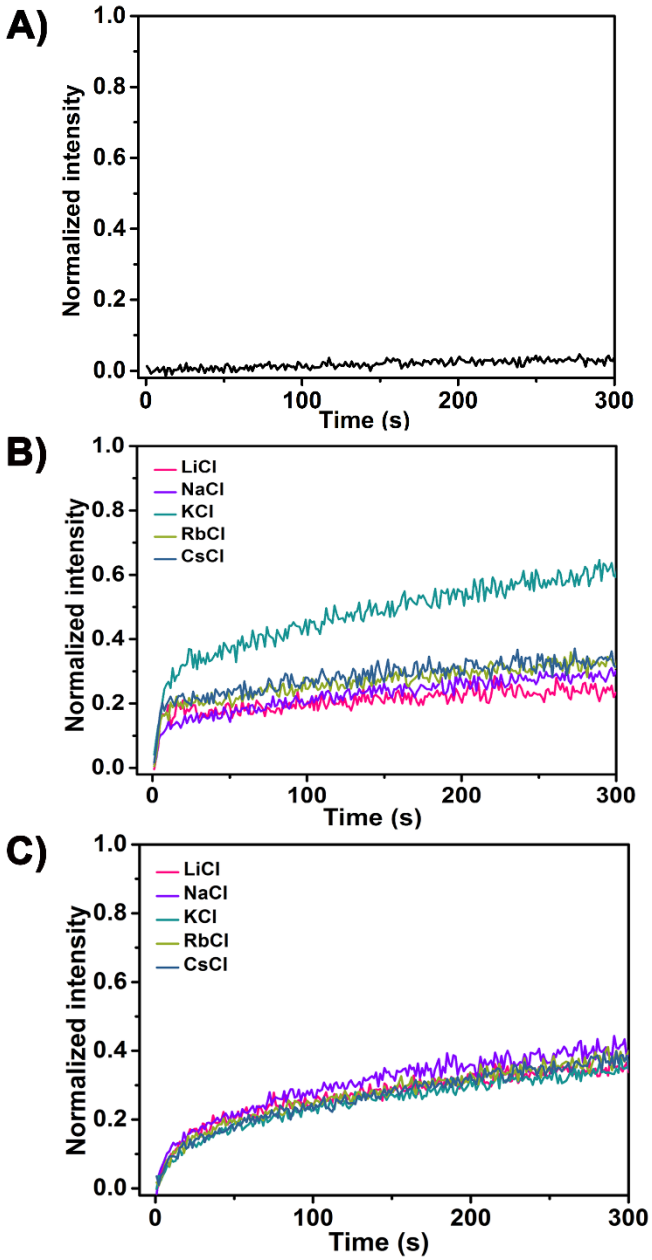

Figure S15 A) The control experiment (addition with 10 μL DMSO) for the cation selectivity. B-C) Cation slectivity assay of B) **[2]rotaxane 3** (3.33 μM) and C) **T3** (13.67 μM), determined by varying extravesicle cations (M^+= Li^+, Na^+, K^+, Rb^+, and Cs^+).

10.3 Anion selectivity.

The procedure was similar as that of cation selectivity except using defferent buffer (10 mM HEPES, 100 mM KX, pH = 7.0, where, X^- = F^-, Cl^-, Br^-, and I^-) as extravesicle solution. The added base was KOH.

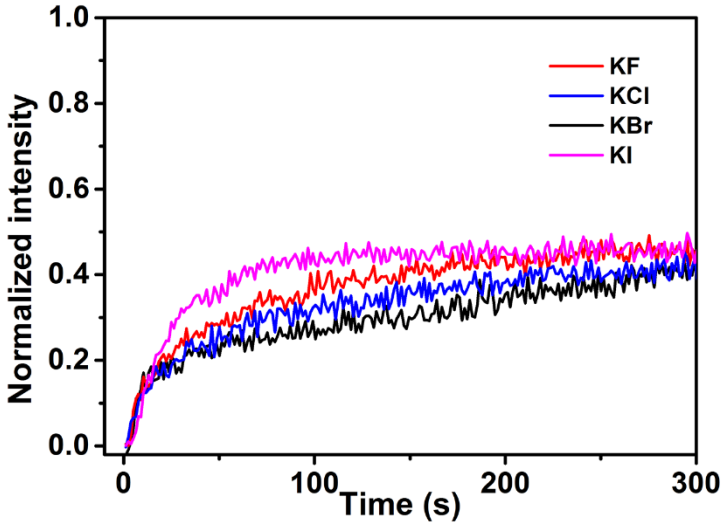

Figure S16 Anion slectivity assay of **[2]rotaxane 3** (0.67 μM) determined by varying extravesicle anions (A^- = F^-, Cl^-, Br^-, and I^-). The control experiment was the same as in **Figure 15**.

10.4 Lucigenin assay.

Preparation of POPC Vesicles. A solution of 360 μL EYPC (EYPC, 25 mg/mL, 9 mg) in deacidified chloroform was mixed with 100 μL of cholesterol (10 mg/mL, 1 mg) in deacidified chloroform. The solvents were evaporated by a slow stream of nitrogen, followed by drying under vacuum for 12 hours. Then the lipid membrane was rehydrated by overtaxing with a 500 μL of salt solution containing of 225 mM $NaNO_3$ and 1 mM N,N'-Dimethyl-9,9'-biacridinium dinitrate (Lucigenin) in 5 mM phosphate buffer (PB, pH=7.2). Then, the suspension was subjected to seven freeze–thaw cycles and allowed to age for 30 min at room temperature before extruding 25 times through a 200 nm polycarbonate membrane. The excess Lucigenin was separated from the vesicles by size exclusion column chromatography (SephadexG-25) using 225 mM $NaNO_3$ PB solution (5 mM, pH=7.2) as eluent. The vesicles were further diluted to reach a total lipid concentration of 0.4 mM, assuming 100% retention of lipid during the gel filtration process.

Lucigenin vesicle fluorescence assay. In a typical experiment, 3 mL of stock EYPC liposomes (0.4 mM) as prepared above were transferred to a quartz cuvette. The temperature was set at 25 ^{o}C, and the sample was left stirring for 2 min in the fluorescence spectrometer in order for the sample to reach the set temperature. The spectrometer used a 368 nm excitation wavelength and measured the fluorescence at 506 nm. At 50 s and 100 s after the start of the measurement, a 100 μL of PB solution containing of 4 M NaCl and 225 mM $NaNO_3$ and 10 μL THF solution containing transporters in different concentrations were respectively added. After 550 s, 100 μL of 5% Triton-X detergent was added to lyse the liposomes. All transport experiments were done in triplicate, and the initial data (initial plateaus and drop by quenching of external Lucigenin, before 50 s) were removed. The detected fluorescent intensity was normalized into $I_F = F/F_0$ (F_0, the fluorescent intensity before the addition of transporter), the solvent THF (10 μL) was also monitored as the fluorescence background.

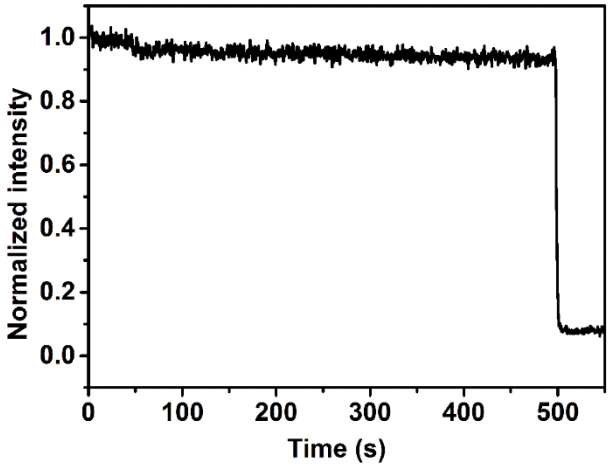

Figure S17 The control experiment (10 μL THF without addition of transporter) for the lucigenin experiment.

10.5 Valinomycin assay.

The vesicles preparation, experimental procedure and data processing were same

as above LUVs⊃HPTS except using different buffer with [Na^+_{in}] = 100 mM and [K^+_{out}] = 100 mM (section 6.2).

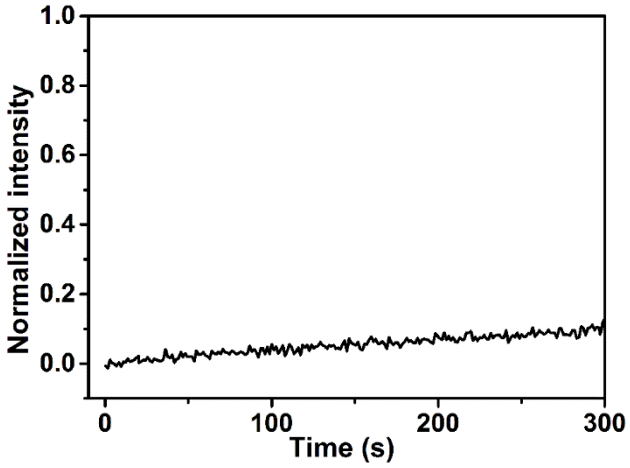

Figure S18 The control experiment (10 μL DMSO without addition of transporter) for the valinomycin experiment.

10.6 Ion selectivity determined by permeability ratios.

For the measurement of the transport selectivity of K^+ over Cl^-, the cis and trans chamber was charged with KCl of 0.3 M and 1.0 M, respectively. The molecular shuttle **[2]rotaxane 3** were added to the cis compartment to reach a final concentration of 5 μM. The selectivity of the molecular shuttle for K^+ over Cl^-, defined as the permeability ratio of two ions, was calculated by using Goldman-Hodgkin-Katz (GHK) equation:

$$\varepsilon_{rev} = RT/F \times \ln\{(P_{K^+}[K^+]_{cis} + P_{Cl^-}[Cl^-]_{tans}) / (P_{K^+}[K^+]_{trans} + P_{Cl^-}[Cl^-]_{cis})\} \quad \text{Equation S7}$$

where ε_{rev} is the reversal potential (the potential of zero current); R is the universal gas constant (8.314 $J.K^{-1}.mol^{-1}$); T the temperature in Kelvin (300 K); F is the Faraday's constant (96485 $C.mol^{-1}$); P is the permeability of **[2]rotaxane 3** for ions.

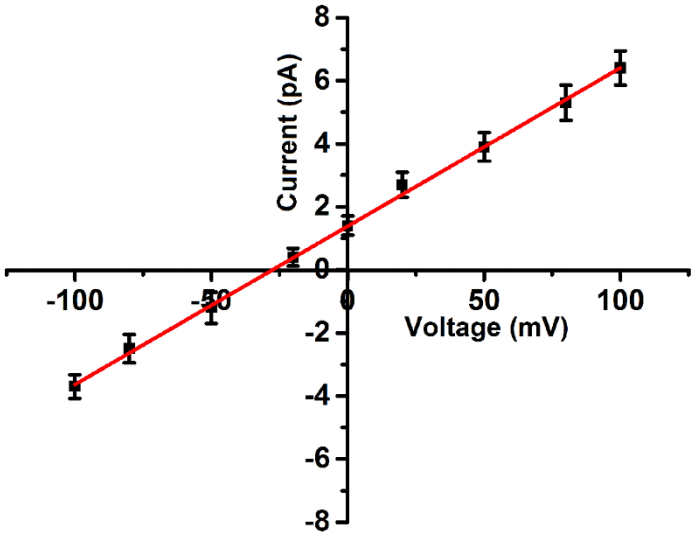

Figure S19 Current-votage relationship of **[2]rotaxane 3** by using unsymmetrial solution at both sides of the bilayer. *Trans* chamber: KCl (1.0 M), *cis* chamber: KCl (0.3 M), the obtained $P_{K^+} / P_{Cl^-} = 28$.

For the measurement of the transport selectivity of Na^+ over K^+, the cis chamber was charged with NaCl (1.0 M) and the trans one was charged with KCl (1.0 M). The molecular shuttle **[2]rotaxane 3** were added to the cis compartment to reach a final concentration of 5 μM. The selectivity of **[2]rotaxane 3** for Na^+ over K^+, defined as the permeability ratio of two ions, was calculated by using the simplified GHK equation since Cl^- transport was ineffective that the permeability of Cl^- can be igored in the GHK equation :

$$P_{Na^+} / P_{K^+} = \exp (\varepsilon_{rev} F / RT) \qquad \text{Equation S8}$$

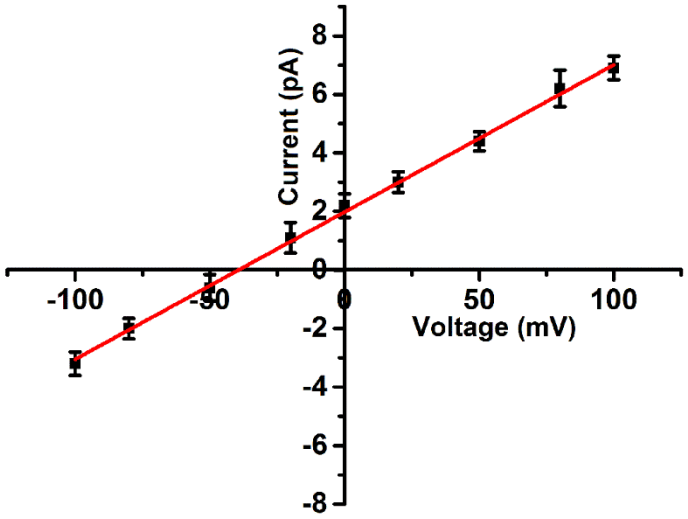

Figure S20 Current-votage relationship of **[2]rotaxane 3** by using unsymmetrial solution at both sides of the bilayer. *Trans* chamber: KCl (1.0 M), *cis* chamber: NaCl (1.0 M), the obtained $P_{Na^+} / P_{K^+} = 0.2$.

11. The comparison of transport activity among the rotaxanes with different stations.

The synthesis of rotaxane **[2]rotaxane 1** and **[2]rotaxane 2** has been described as in Scheme S4 and S5.

11.1 The shuttling rate calculation of [2]rotaxane 2 from 2D-EXSY.

The 2D-EXSY NMR spectrum (600 MHz, 298 K, $\tau_m = 500$ ms) of **[2]rotaxane 2** is shown in Figure S21 (The detailed experimental process was same as described in Section 4). No obvious cross-peaks were observed even at $\tau_m = 500$ ms, it indicated a slower shuttling rate for **[2]rotaxane 2**. Although the shuttling rate can't be estimated by 2D-EXSY experiments, the shuttling motion of **[2]rotaxane 2** undoubtedly exists by Brownian motion.

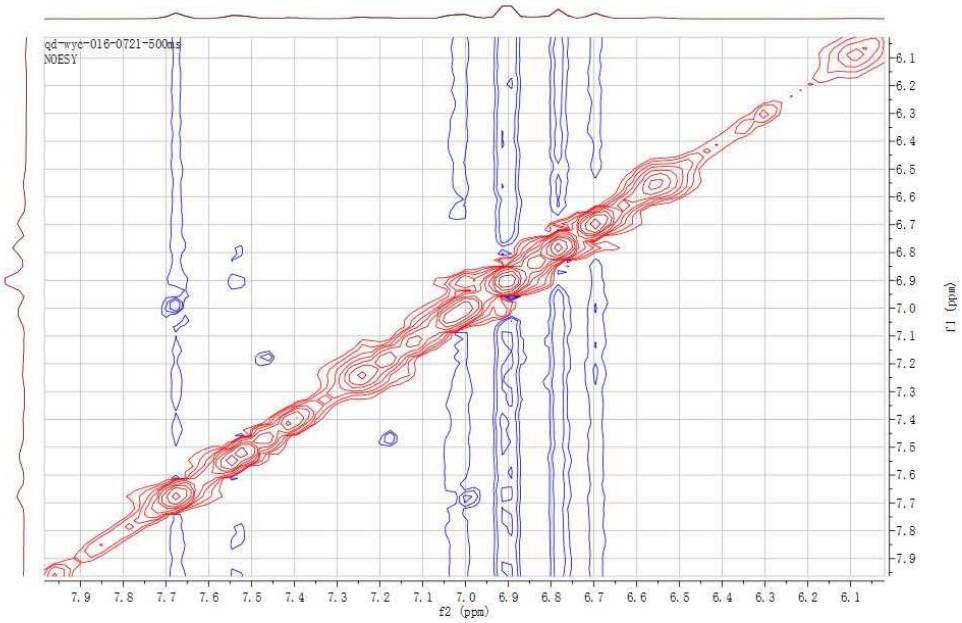

Figure S21 2D EXSY NMR spectrum (600 MHz, 298 K, τ_m = 500 ms) of **[2]rotaxane 2** at 20 mM in CD_3CN / $CDCl_3$ (v / v, 1 / 1).

11.2 The comparison of the transport activity of the rotaxanes.

The transport activity assay was similar as described in section 6.2.

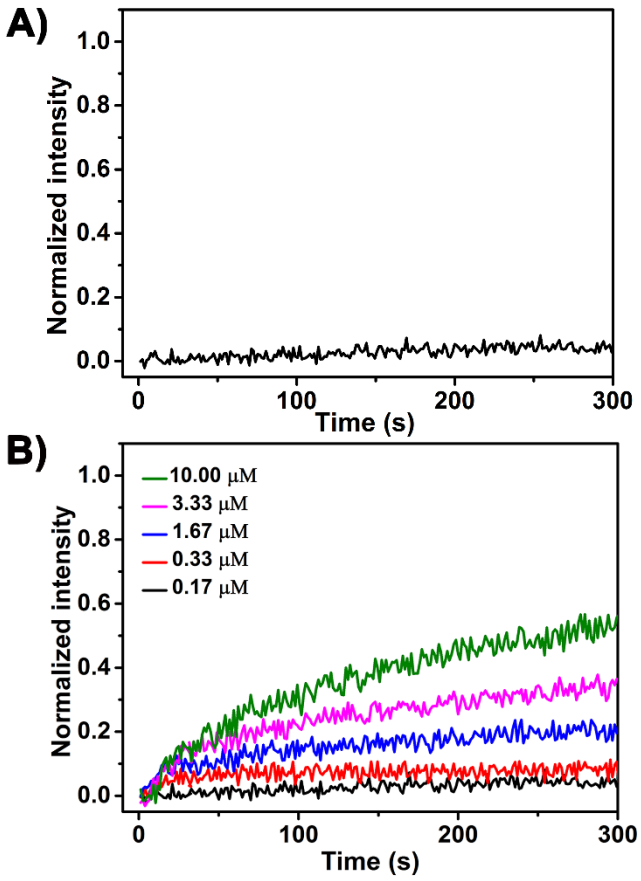

Figure S22 A) The fluorescent evolution of the control experiment (addition with 10

μL DMSO). B) Concentration-dependent enhancement of ion transport activity of **[2]rotaxane 2** using10 mM HEPES, 100 mM KCl, pH = 7.0 as external buffer.

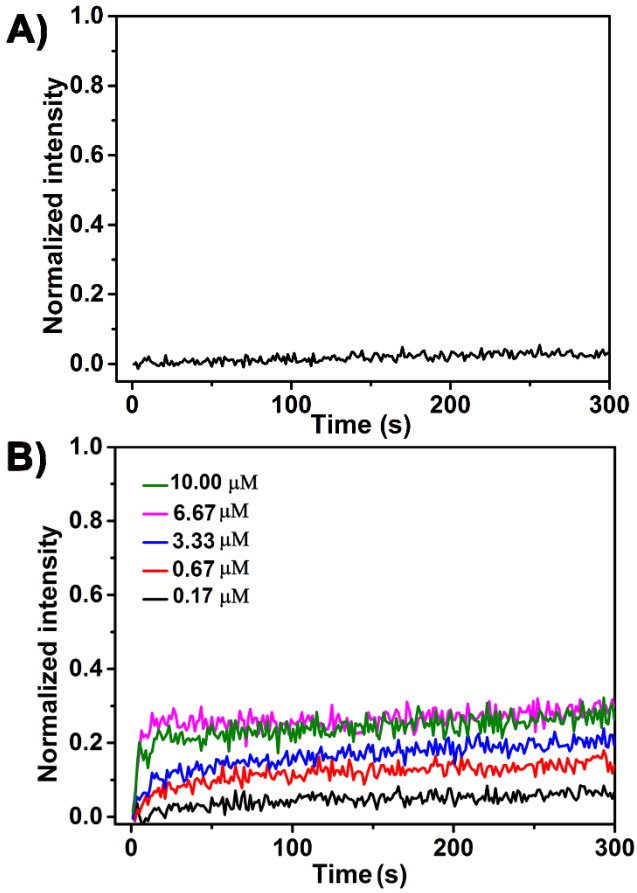

Figure S23 A) The fluorescent evolution of the control experiment (addition with 10 μL DMSO). B) Concentration-dependent enhancement of ion transport activity of **[2]rotaxane 1** using10 mM HEPES, 100 mM KCl, pH = 7.0 as external buffer.

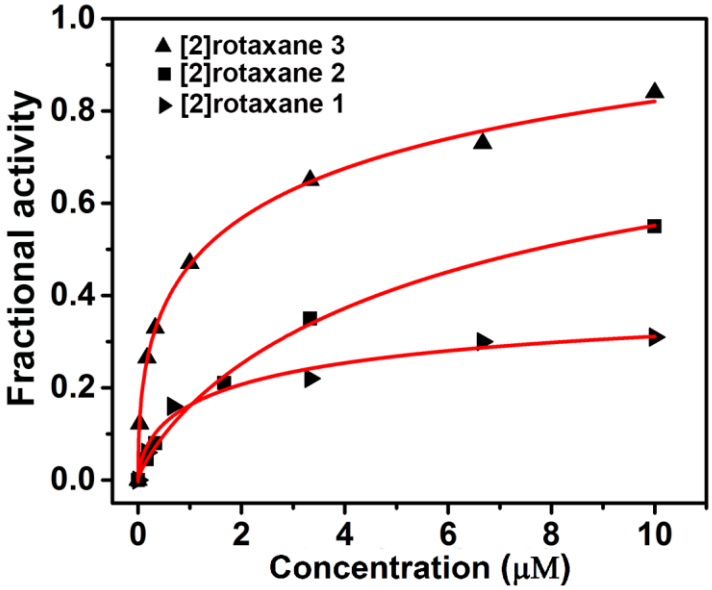

Figure S24 The comparison of transmembrane activities (t = 300 s) among **[2]rotaxane 3**, **[2]rotaxane 2** and **[2]rotaxane 1** at different concentrations. The red lines were the

fitted curves from Logistic regression equation.

11.3 The comparison of the transport activity of the threads.

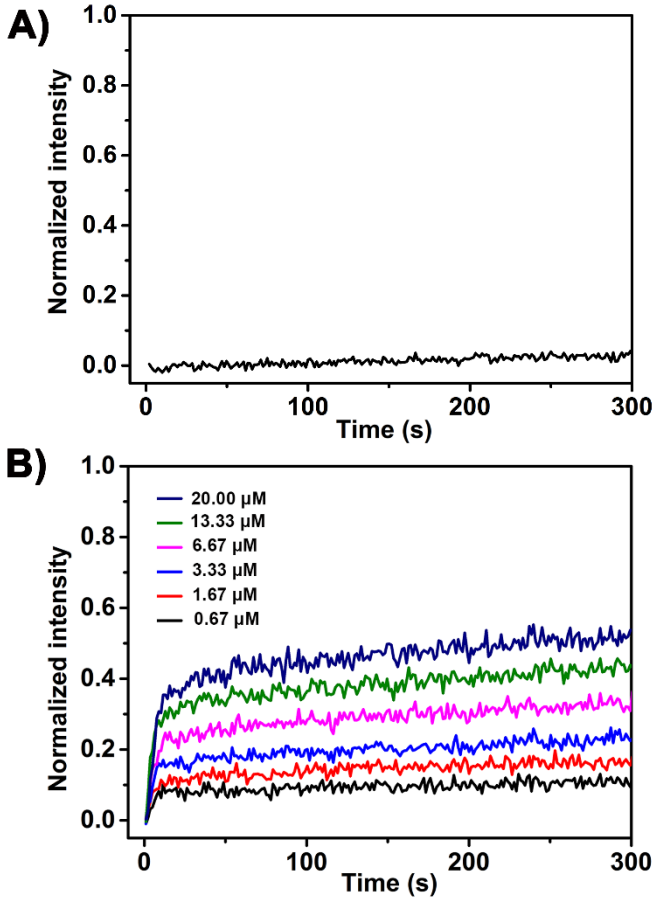

Figure S25 A) The fluorescent evolution of the control experiment (addition with 10 μL DMSO). B) Concentration-dependent enhancement of ion transport activity of **T2** using10 mM HEPES, 100 mM KCl, pH = 7.0 as external buffer.

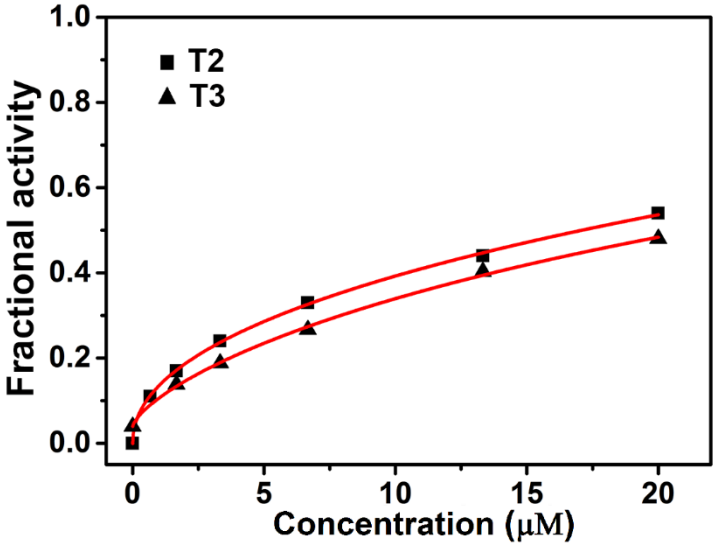

Figure S26 The comparison of transmembrane activities (t = 300 s) between **T3** and **T2** at different concentrations. The red lines were the fitted curves from Logistic

regression equation.

12. Investigation of pH effects on ion transport.

12.1 The ^{1}H NMR spectra of [2]rotaxane 3 in different pH values.

A solution of **[2]rotaxane 3** was prepared in the stated deuterated solvents (of the order of 5 mM) into the NMR tube. The ^{1}H NMR spectrum was sequentially recorded with addition of 0, 1.2 and 2.4 equivalent of 1,8-diazabicyclo[5.4.0]undec-7-ene (DBU). As shown in Figure S27, in the absence of DBU (0 eq DBU), there are two sets of peaks at 6.62 ppm and 6.78 ppm for the aromatic H_a and $H_{a'}$, respectively, which could be clearly assigned as complexed and uncomplexed thread protons and underwent slow exchange at 298 K. With the addition of DBU, the splitted peaks of H_a and $H_{a'}$ began to merge, the proton H_d was downshifted and the proton of H_f and H_g was upshifted. It was resulted from the deprotonation of two ammonium stations and the static recognition of wheel at the MTA station under basic condition. All these indicated that the molecular shuttle of **[2]rotaxane 3** can be affected by acid-base drive.

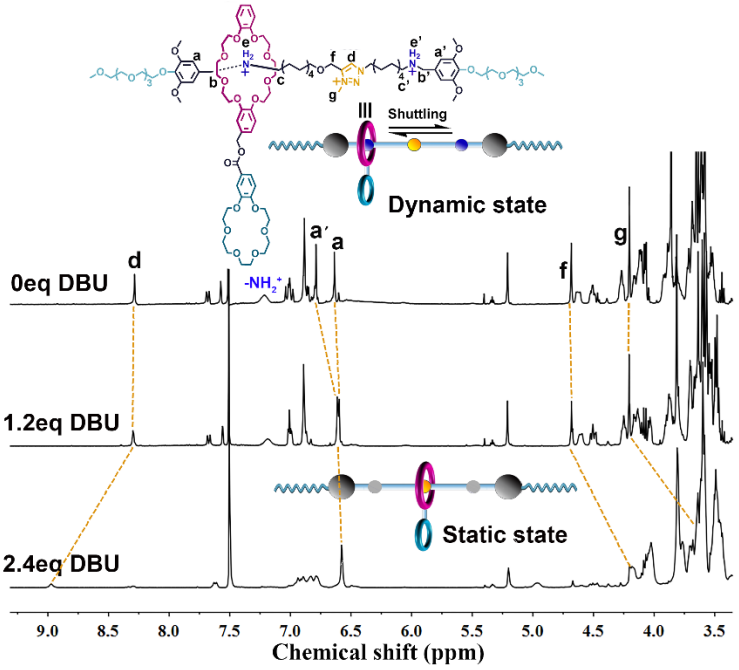

Figure S27 ^{1}H NMR of **[2]rotaxane 3** in $CDCl_3$ / CD_3CN (v / v, 1 / 1) with additions of organic base DBU, Up: 0 eq, Middel: 1.2 eq, and Down: 2.4 eq.

12.2 ^{23}Na NMR spectroscopy experiments at different pH.

Form the pH variable ^{1}H NMR of **[2]rotaxane 3**, it can be concluded that the increase of pH would deprotonate the ammonium sites, thus drive the wheel to locate on the N-methyltriazolium site from which the shuttle motion would be stopped. If the shuttling mechanism plays a key role on the ion transport as expected, the increased pH would decrease and even block the transport of ions. Therefore, ^{23}Na NMR spectroscopy was used to assay the influence of pH on Na^+ transport mediated by **[2]rotaxane 3**. The mechanism of ^{23}Na NMR spectroscopy for the ion transport was originated from the addition of Dy^{3+} shift regent, which was used to differentiate external Na^+ (around -8 ppm) from internal Na^+ (0 ppm). Na^+ transport by the rotaxane was visualized by the line broadening observed for the Na^+ resonances due to the exchange of the internal and external sodium ions.

Preparation of EYPC LUVs: A solution of EYPC lipids (800 μL in chloroform, 25 mg/mL) was concentrated under a slow stream of nitrogen and then in vacuo for 12 hours to obtain a transparant lipid membrane in bottom. Then, the lipid membrane was hydrated by overtaxing with 1000 μL buffer (Buffer one: 50 mM tris(hydrox-ymethyl) aminomethane, 200 mM NaCl, pH = 7.0; Buffer two: 50 mM 3-(cyclohexyla-mino)-2-hydroxy-1-propanesulfonic acid, 200 mM NaCl, pH = 10.2), and the resulting suspendion was incubated at room temperature for 30 min. The suspension was subjected to seven freeze–thaw cycles to obtain a homogenous solution. Subsequently, the solution was extruded (25 times, 1 mL at a time) through a 100 nm polycarbonate

membrane to finally give the large unilamellar vesicle (LUVs) solution.

Preparation of shift reagent: The shift reagent was prepared by mixing aqueous sodium tris(polyphosphate)solution (2.0 mL, 0.2 M) with aqueous $DyCl_3$ solution (1.0 mL, 0.1 M).

NMR spectroscopy experiment: Samples for acquiring NMR data were prepared in freshly ampules (1.5 mL). The LUVs suspension (450 μL) was first added to the vial followed by a solution of transporter **[2]rotaxane 3** in DMSO (30 μL, 0.13 mM, final concentration). The solution was incubated at room temperature for 45 min before D_2O (100 μL) and the shift reagent (100 μL) were added. The solution was incubated at room temperature for an additional 45 min and then transferred to the NMR tubes. For the blank experiment, the same procedure was used except pure DMSO (30 μL) was added instead of a DMSO solution of **[2]rotaxane 3** .

The line widths for internal Na^+ was detected and compared, which determined the rates for sodium exchange.

Table S2. Peak widths for internal Na^+ in ^{23}Na NMR spectra.

Samples	pH	Peak width (ppm)[a]
[2]rotaxane 3	7.0	3.95
[2]rotaxane 3	10.2	0.39
DMSO	7.0	0.21
[a]the resonance signal for Na^+ inside the vesicle, determined using Top Spin software.		

13. Appendix: ^{1}H NMR, ^{13}C NMR and Mass spectra for New Compounds

(Figure S28-63).

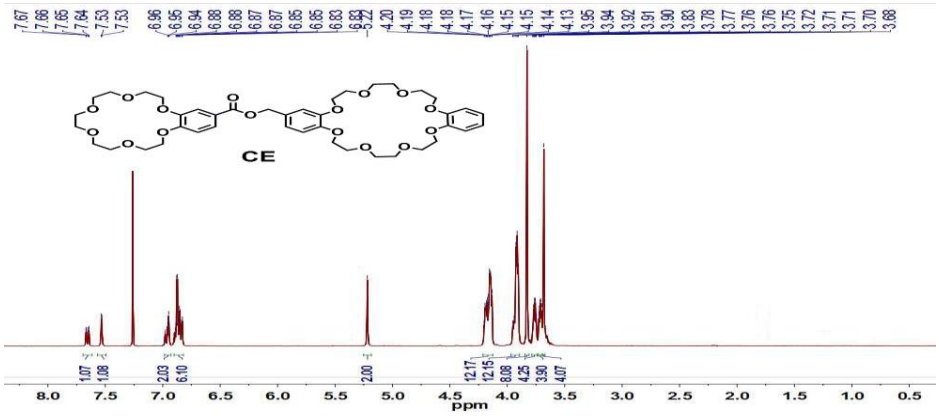

Figure S28 ^{1}H NMR spectrum (400 MHz, $CDCl_3$) of **CE.**

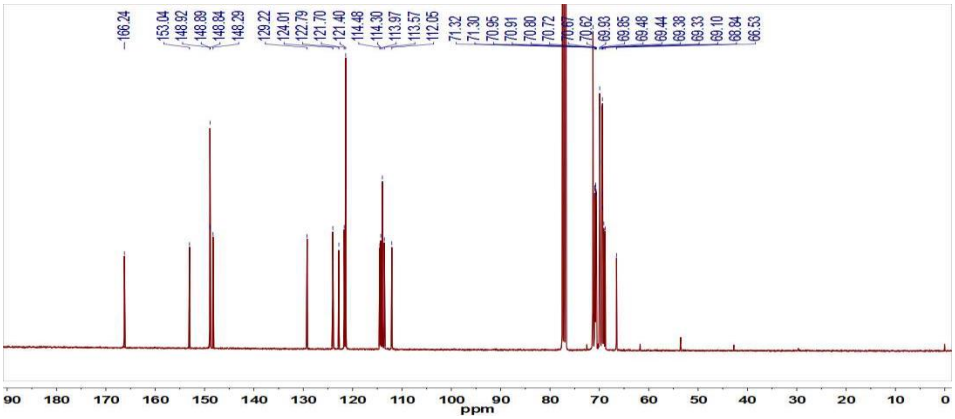

Figure S29 ^{13}C NMR spectrum (100 MHz, $CDCl_3$) of **CE**.

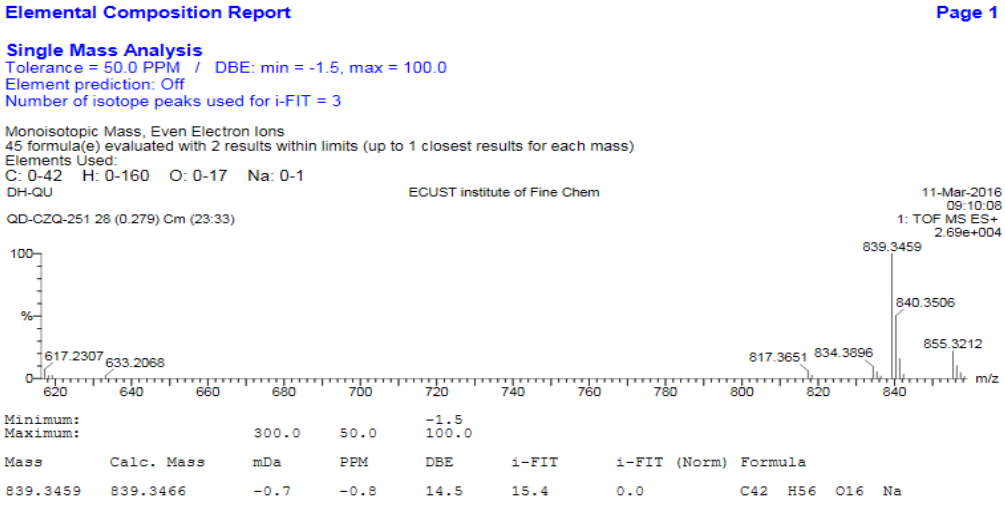

Figure S30 HR-ESI spectrometry of **CE**.

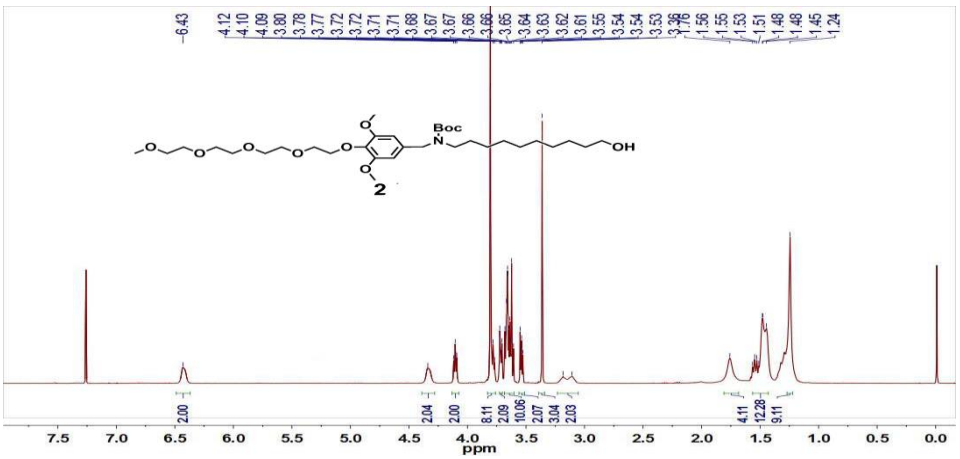

Figure S31 ^{1}H NMR spectrum (400 MHz, $CDCl_3$) of compound **2**.

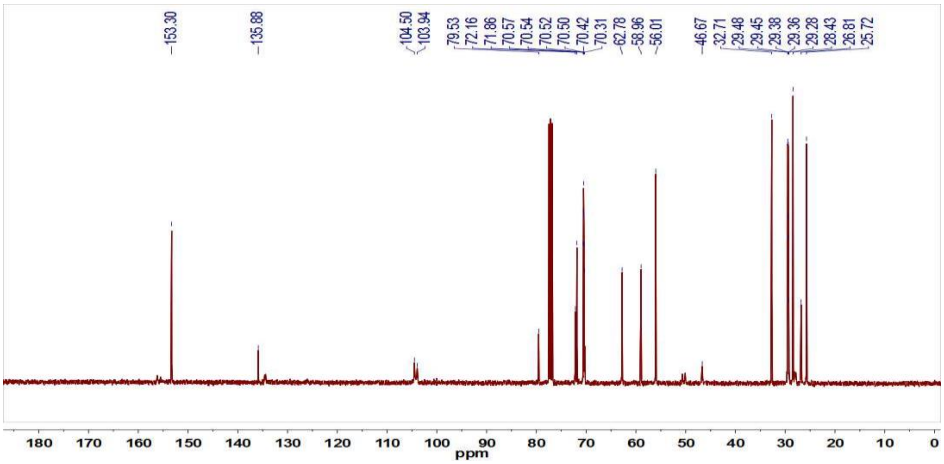

Figure S32 ^{13}C NMR spectrum (100 MHz, $CDCl_3$) of compound **2**.

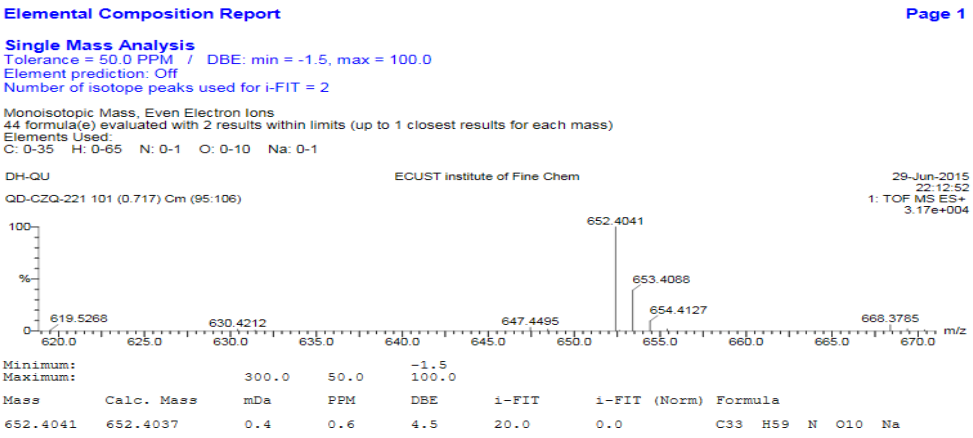

Figure S33 HR-ESI spectrometry of compound **2**.

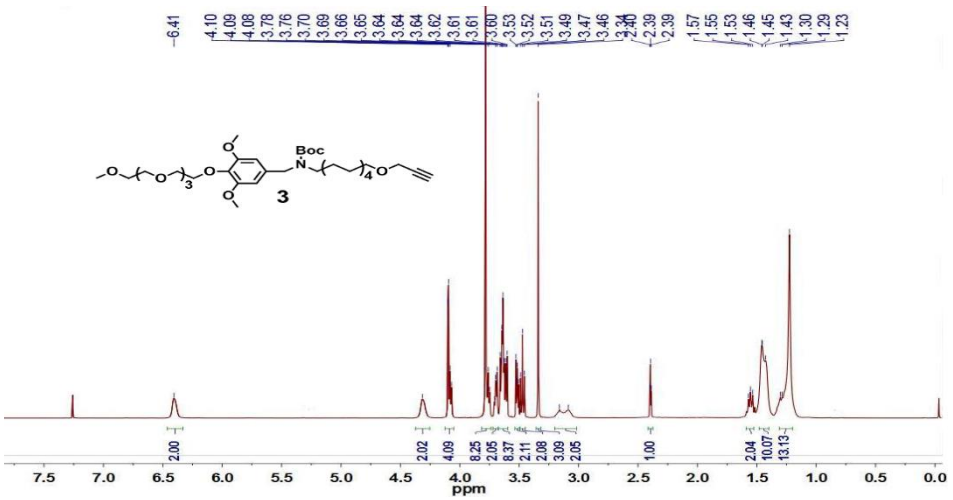

Figure S34 ^{1}H NMR spectrum (400 MHz, $CDCl_3$) of compound **3**.

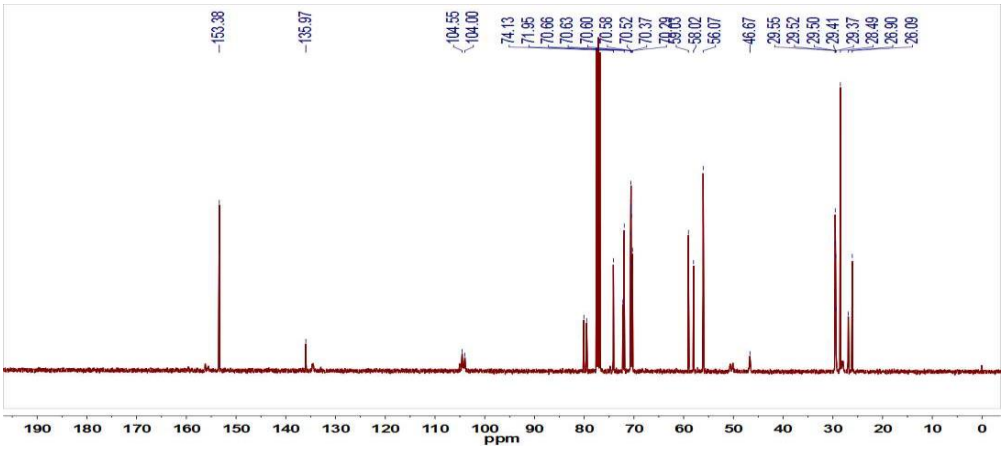

Figure S35 ^{13}C NMR spectrum (100 MHz, $CDCl_3$) of compound **3**.

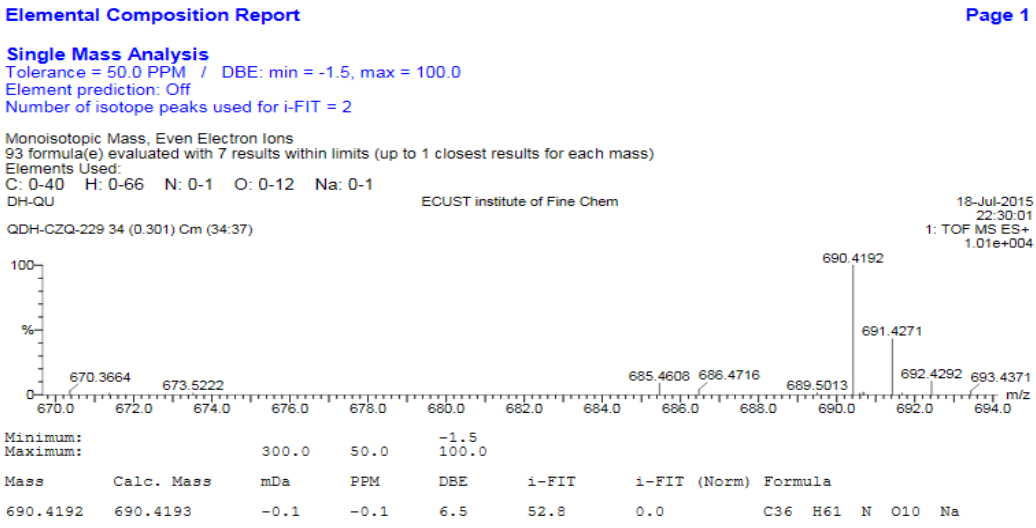

Figure S36 HR-ESI spectrometry of compound **3**.

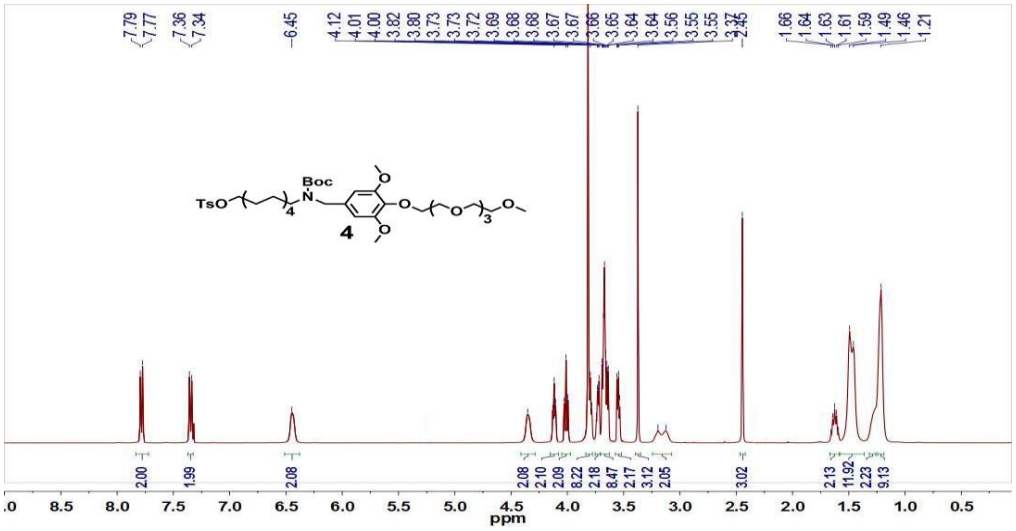

Figure S37 ^{1}H NMR spectrum (400 MHz, $CDCl_3$) of compound **4**.

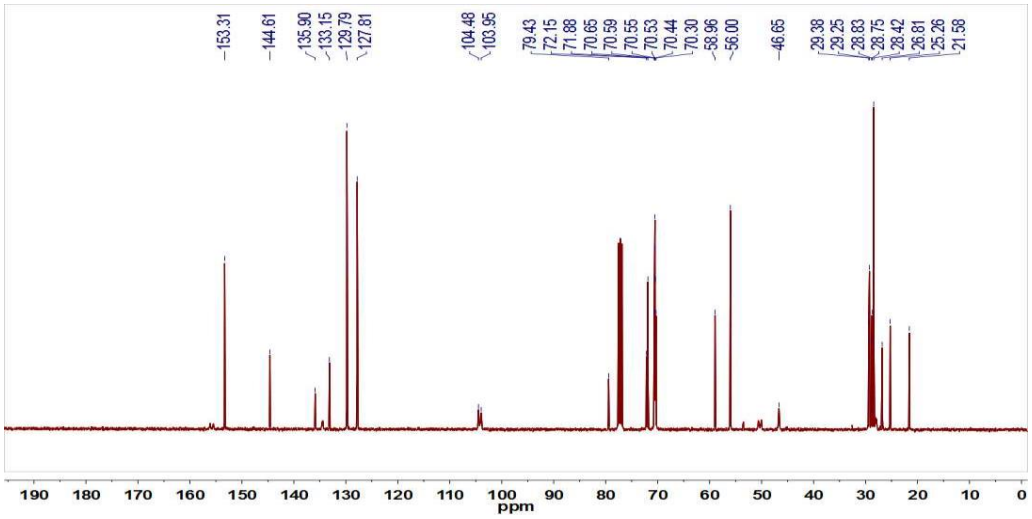

Figure S38 ^{13}C NMR spectrum (100 MHz, $CDCl_3$) of compound **4**.

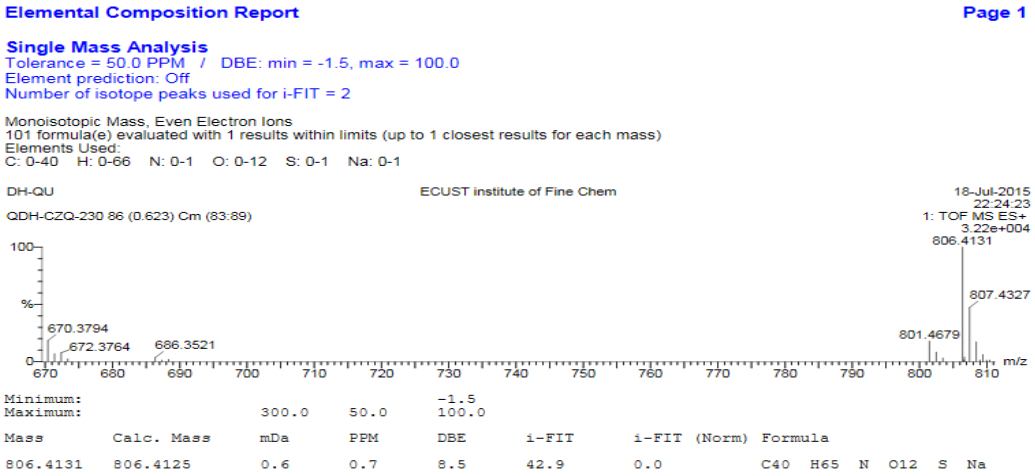

Figure S39 HR-ESI spectrometry of compound **4**.

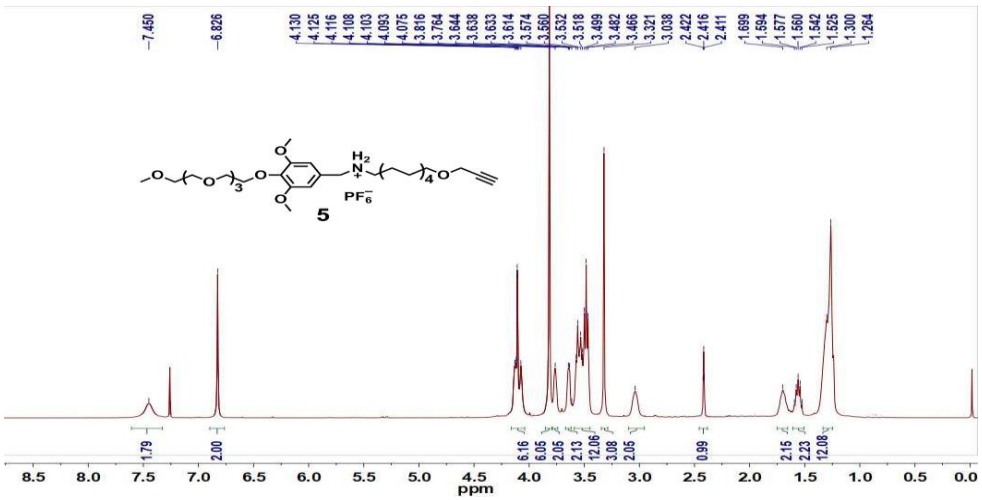

Figure S40 ^{1}H NMR spectrum (400 MHz, $CDCl_3$) of compound **5**.

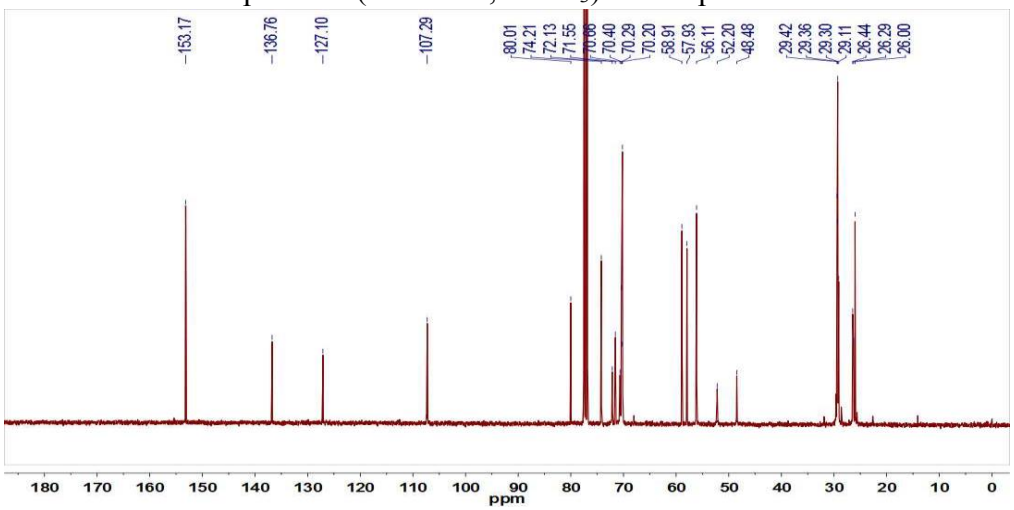

Figure S41 ^{13}C NMR spectrum (100 MHz, $CDCl_3$) of compound **5**.

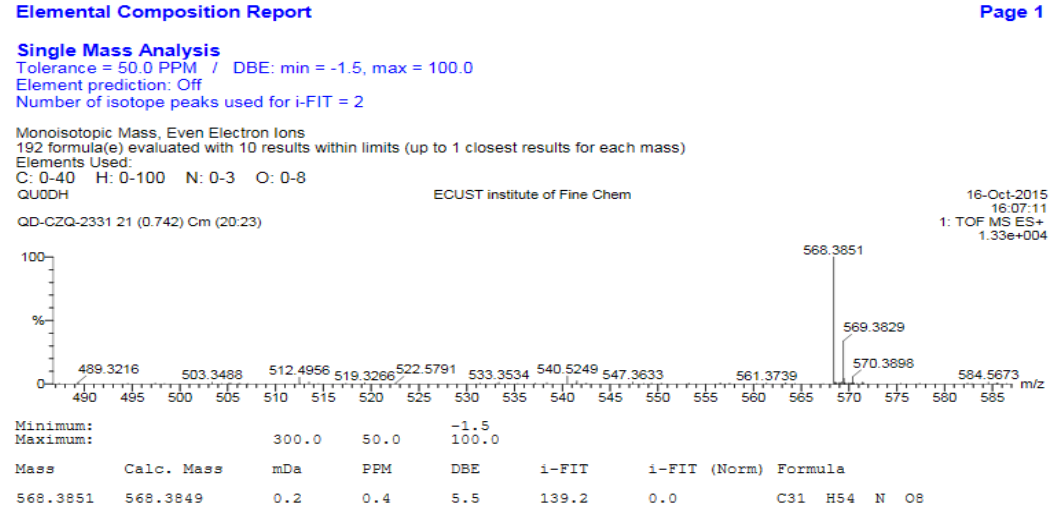

Figure S42 HR-ESI spectrometry of compound **5**.

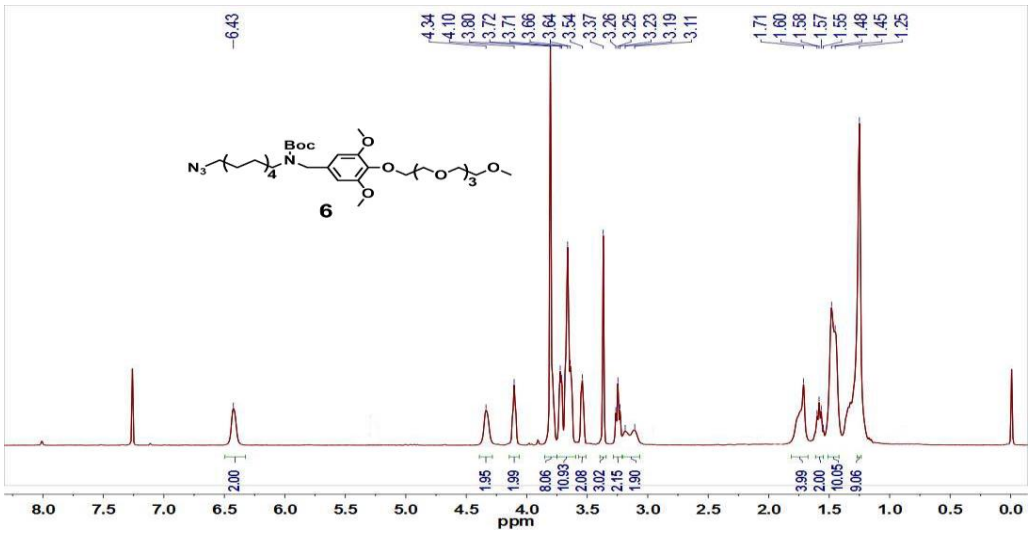

Figure S43 ^{1}H NMR spectrum (400 MHz, $CDCl_3$) of compound **6**.

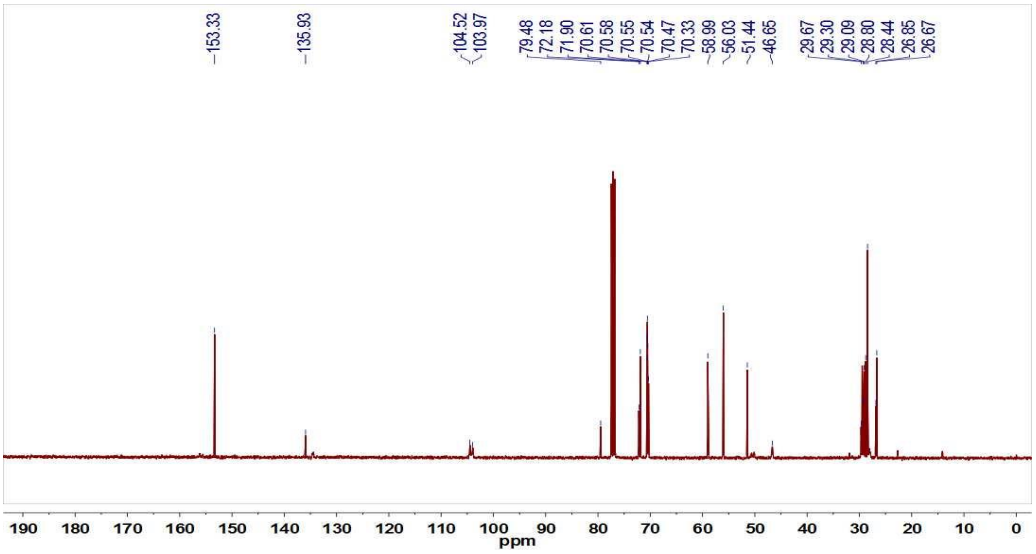

Figure S44 ^{13}C NMR spectrum (100 MHz, $CDCl_3$) of compound **6**.

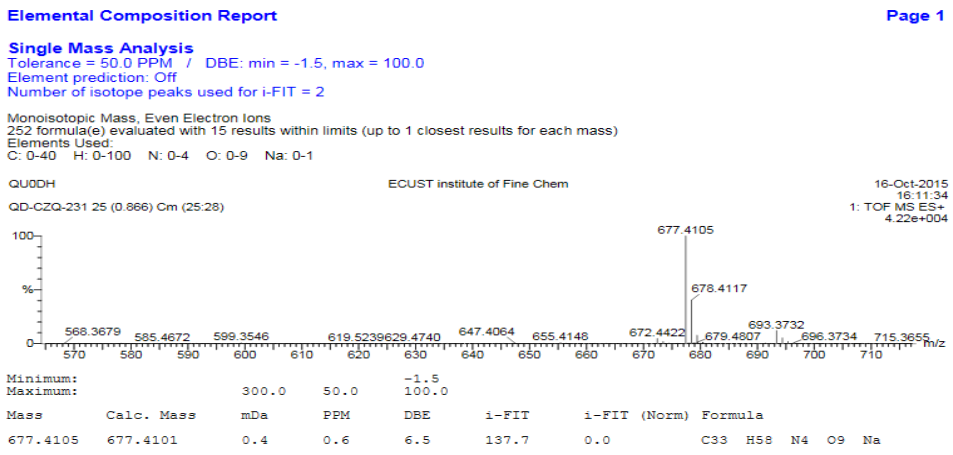

Figure S45 HR-ESI spectrometry of compound **6**.

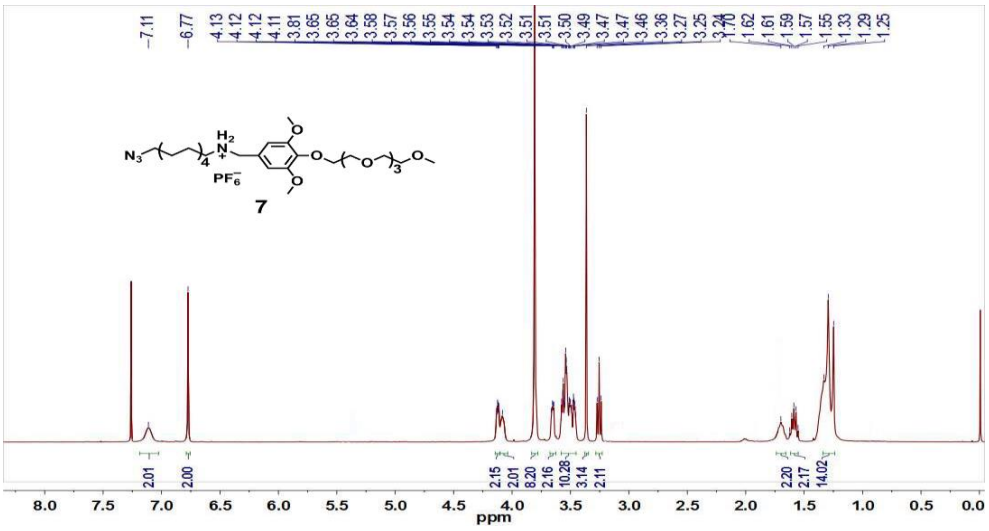

Figure S46 ^{1}H NMR spectrum (400 MHz, $CDCl_3$) of compound **7**.

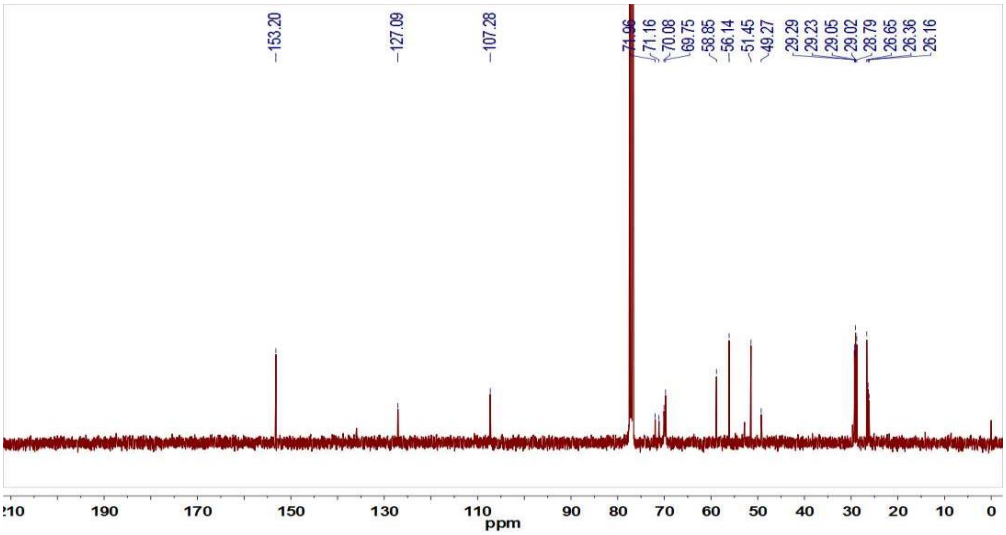

Figure S47 ^{13}C NMR spectrum (100 MHz, $CDCl_3$) of compound **7**.

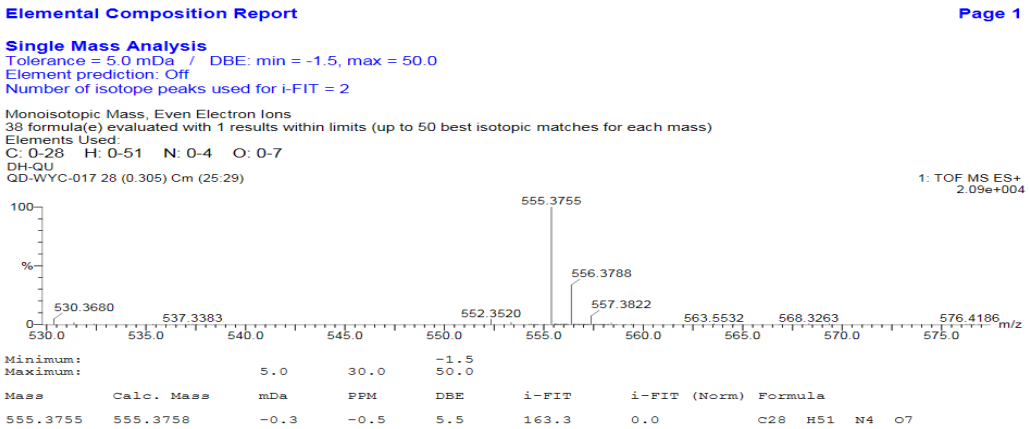

Figure S48 HR-ESI spectrometry of compound **7**.

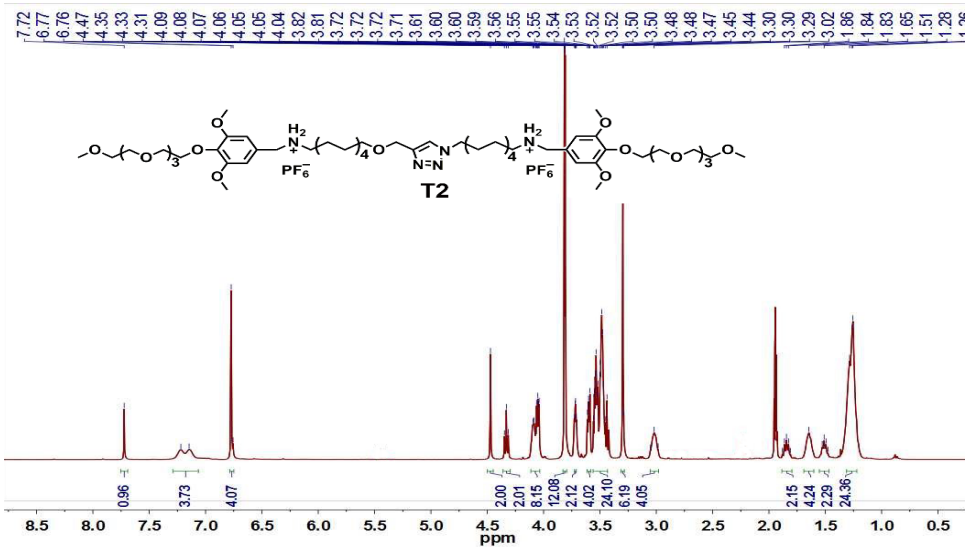

Figure S49 ^{1}H NMR spectrum (400 MHz, CD_3CN) of compound **T2**.

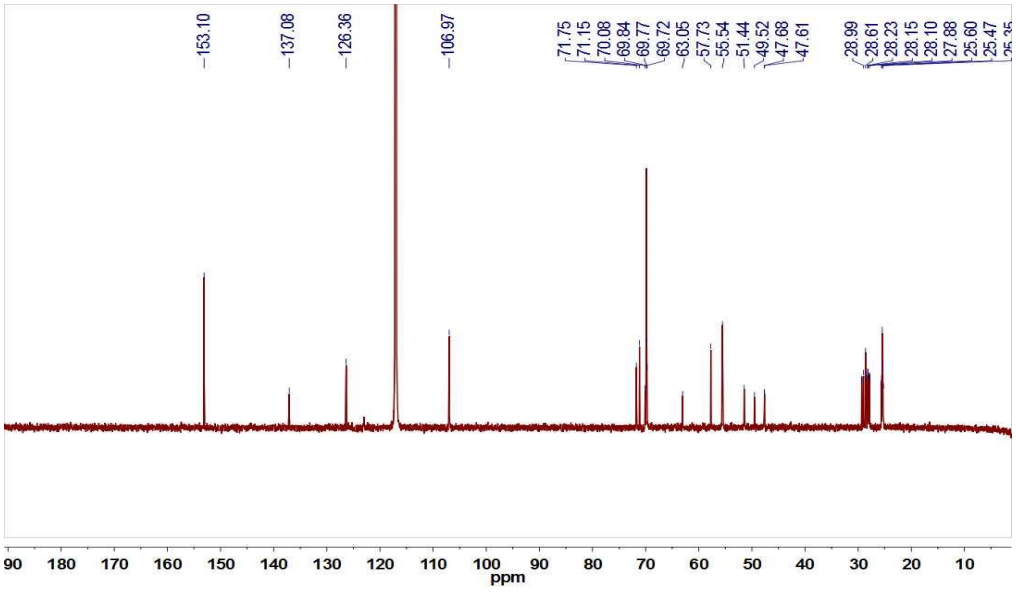

Figure S50 ^{13}C NMR spectrum (100 MHz, CD_3CN) of compound **T2.**

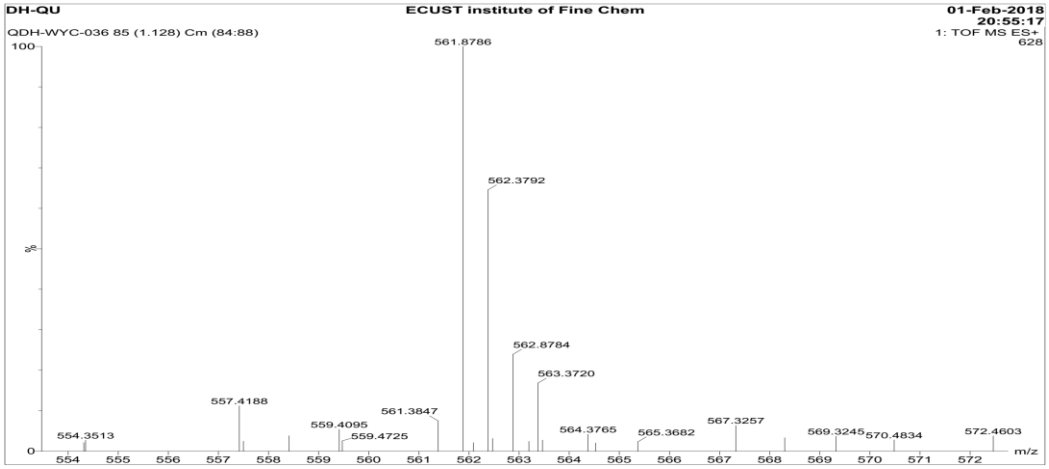

Figure S51 HR-ESI spectrometry of compound **T2**.

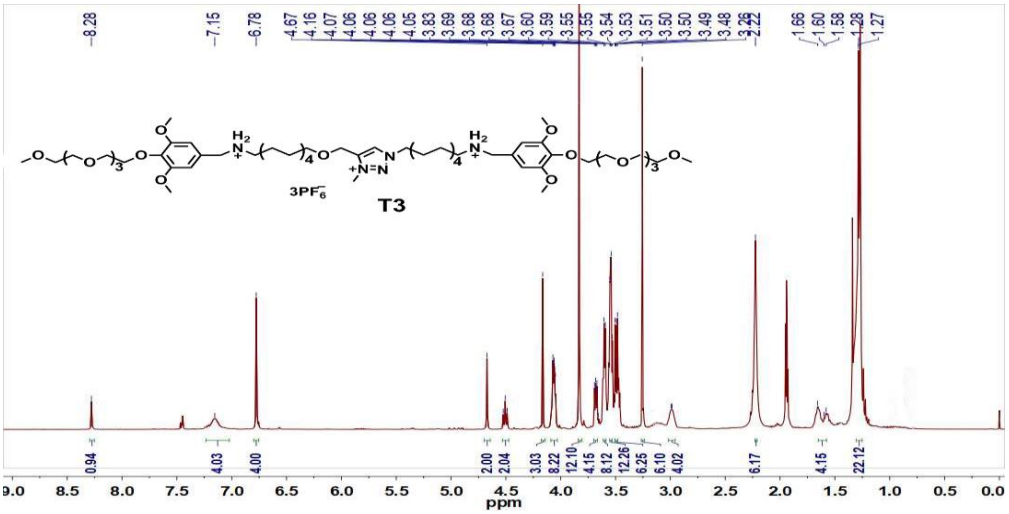

Figure S52 ^{1}H NMR spectrum (400 MHz, CD_3CN) of compound **T3**.

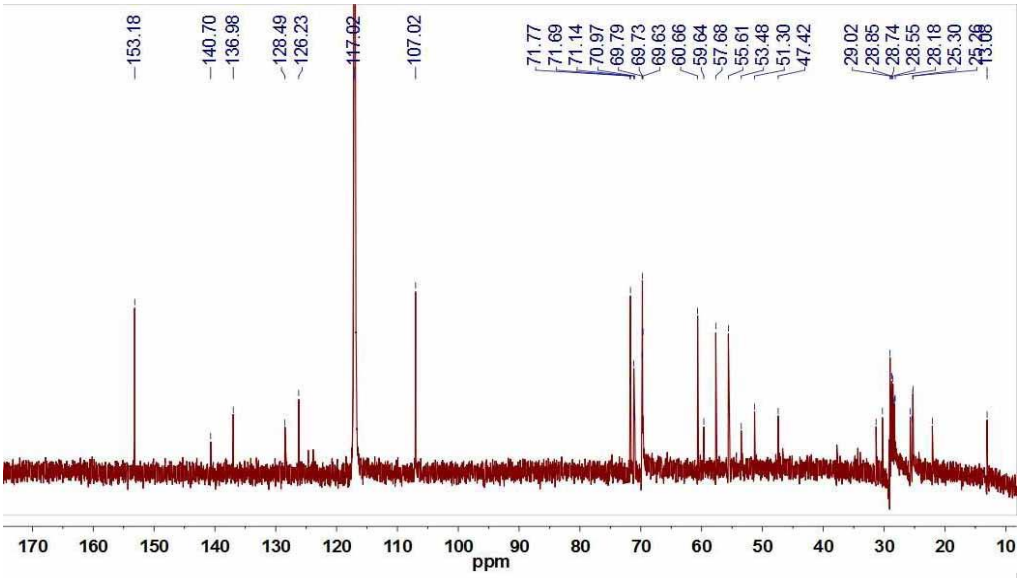

Figure S53 ^{13}C NMR spectrum (100 MHz, CD_3CN) of compound **T3**.

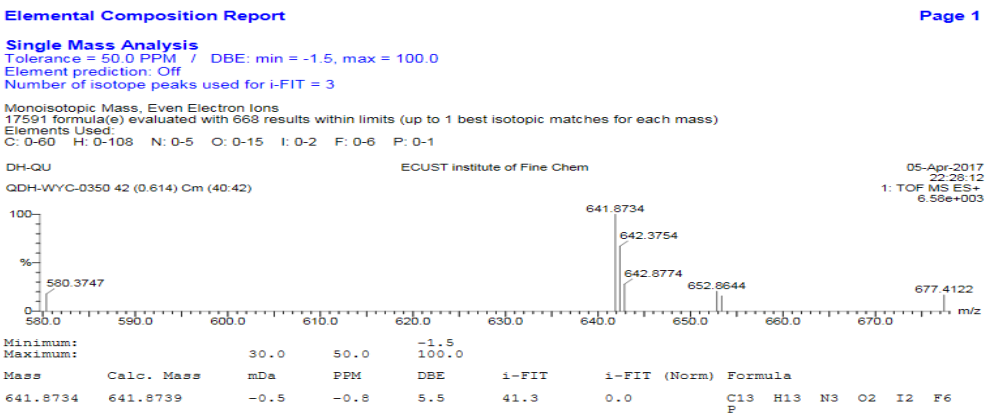

Figure S54 HR-ESI spectrometry of **compound T3**.

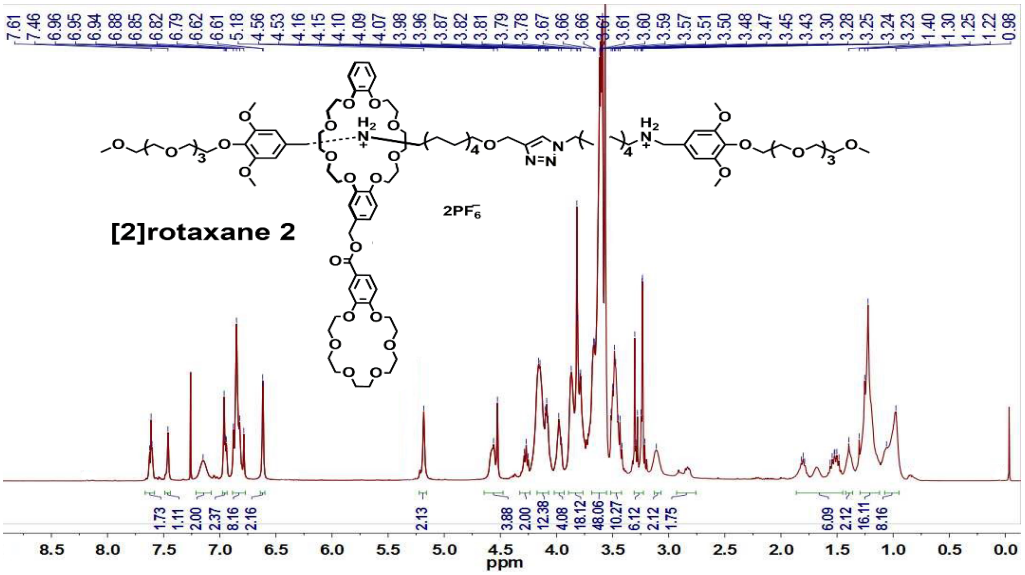

Figure S55 ^{1}H NMR spectrum (400 MHz, $CDCl_3$, 298 K) of **[2]rotaxane 2**.

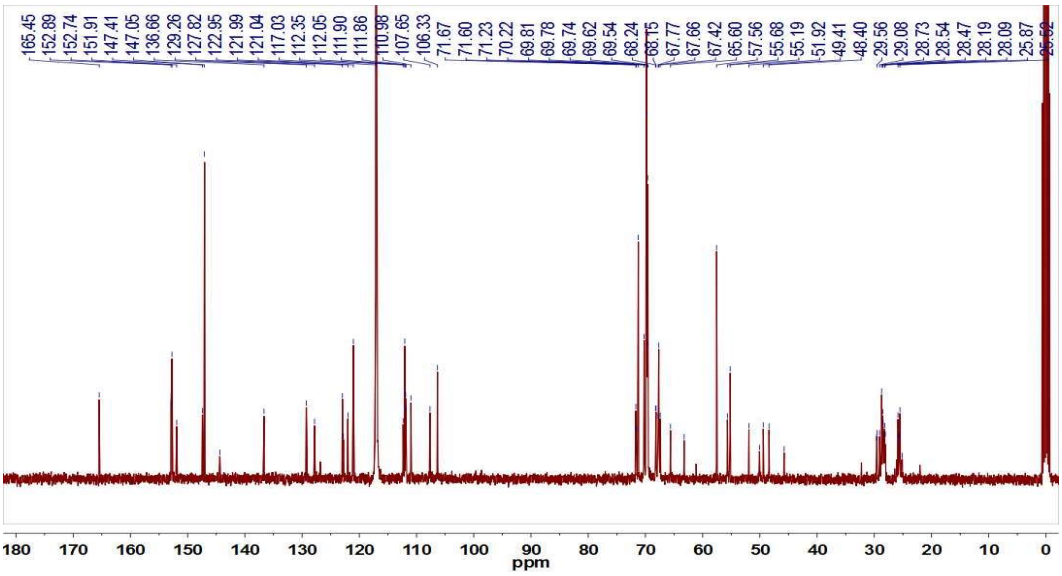

Figure S56 ^{13}C NMR spectrum (100 MHz, CD_3CN, 298 K) of **[2]rotaxane 2**.

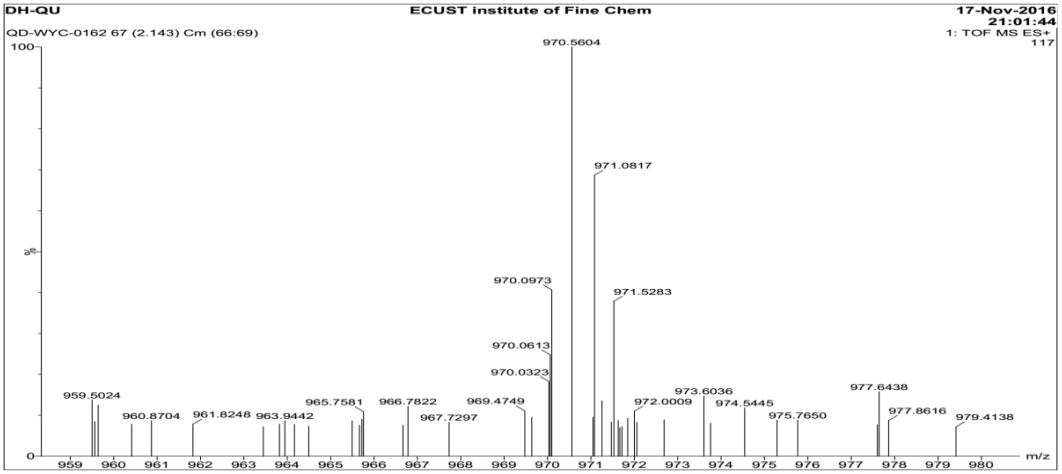

Figure S57 HR-ESI spectrometry of **[2]rotaxane 2**.

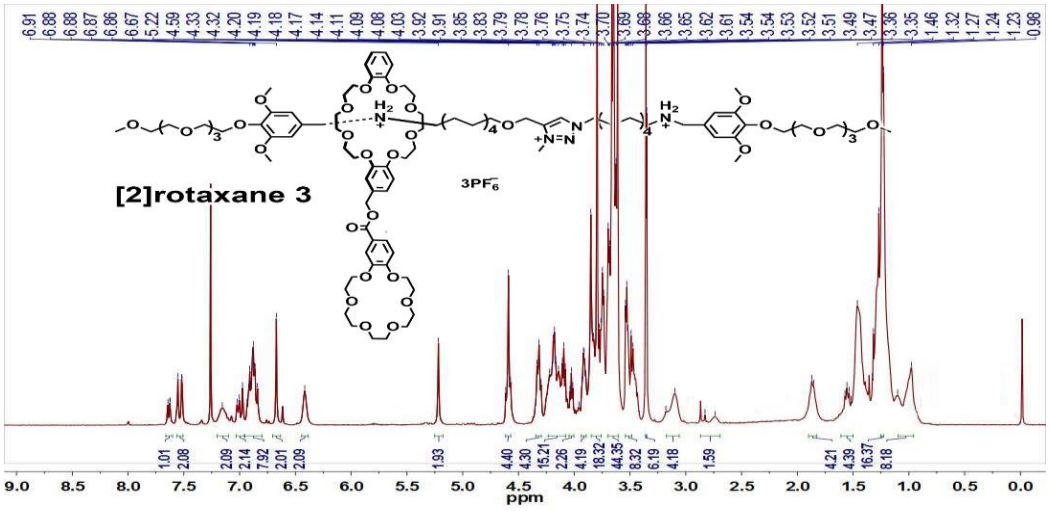

Figure S58 ^{1}H NMR spectrum ($CDCl_3$, 400 MHz, 298 K) of **[2]rotaxane 3**.

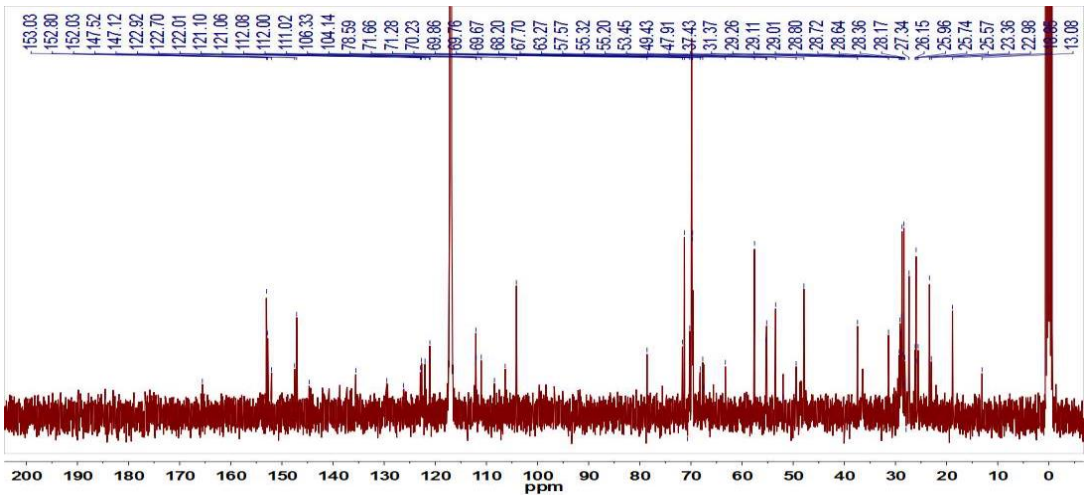

Figure S59 ^{13}C NMR spectrum (CD_3CN, 100 MHz, 298 K) of **[2]rotaxane 3**.

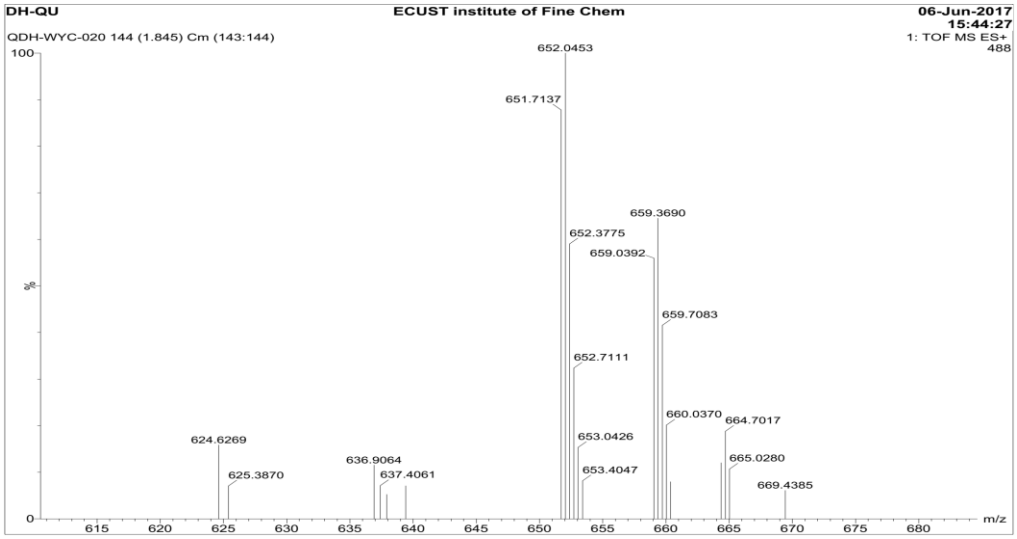

Figure S60 HR-ESI spectrometry of **[2]rotaxane 3**.

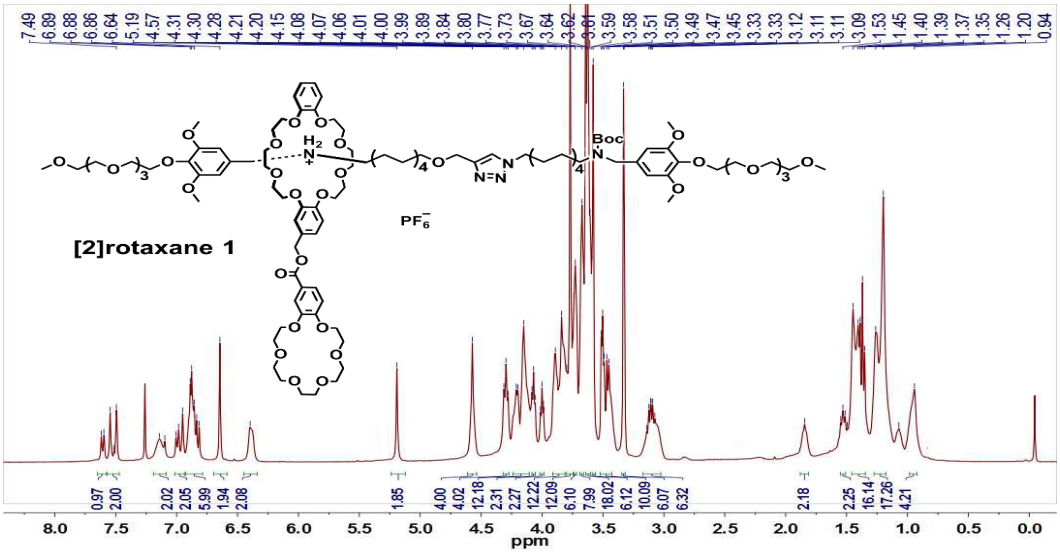

Figure S61 ^{1}H NMR spectrum ($CDCl_3$, 400 MHz, 298 K) of **[2]rotaxane 1**.

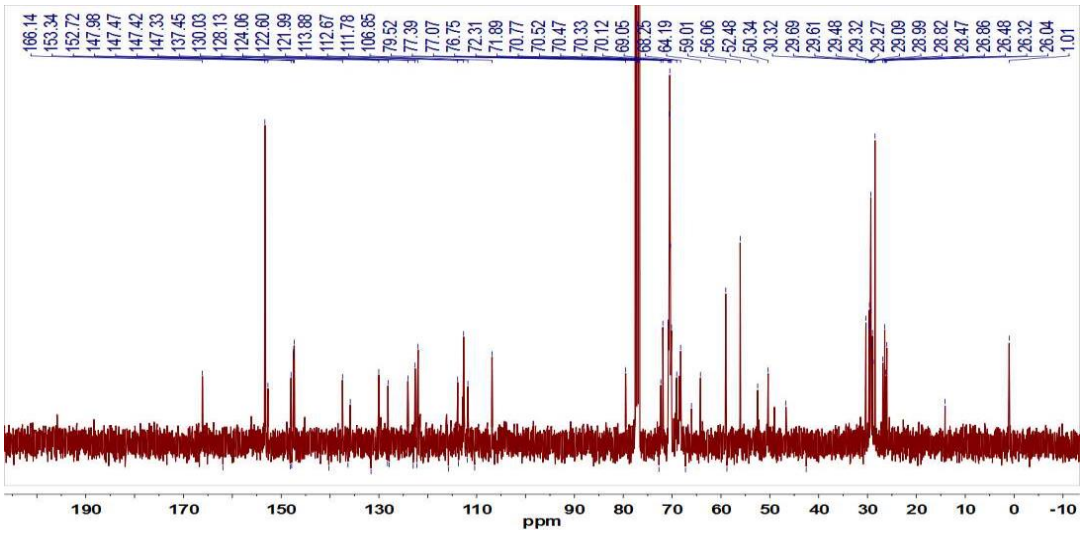

Figure S62 ^{13}C NMR spectrum ($CDCl_3$, 100 MHz, 298 K) of **[2]rotaxane 1**.

Elemental Composition Report **Page 1**

Single Mass Analysis
Tolerance = 50.0 PPM / DBE: min = -1.5, max = 100.0
Element prediction: Off
Number of isotope peaks used for i-FIT = 3

Monoisotopic Mass, Even Electron Ions
193 formula(e) evaluated with 1 results within limits (up to 1 best isotopic matches for each mass)
Elements Used:
C: 0-106 H: 0-168 N: 0-5 O: 0-33

DH-QU ECUST institute of Fine Chem 17-May-2017 17:24:20
QD-WYC-018 19 (0.336) Cm (18:20) 1: TOF MS ES+ 8.43e+003

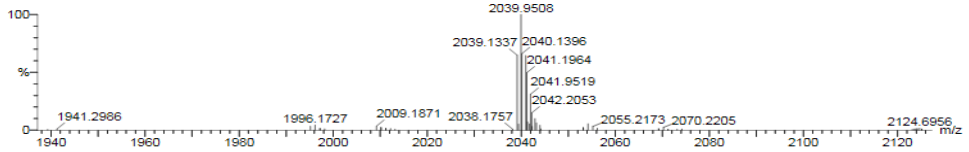

Minimum:				-1.5			
Maximum:		30.0	50.0	100.0			
Mass	Calc. Mass	mDa	PPM	DBE	i-FIT	i-FIT (Norm)	Formula
2039.1337	2039.1622	-28.5	-14.0	25.5	88.6	0.0	C106 H168 N5 O33

Figure S63 HR-ESI spectrometry of **[2]rotaxane 1**.

14. Reference.

(1) Liu, D.; Wang, D. P.; Wang, M.; Zheng, Y. J.; Koynov, K.; Auernhammer, G. K.; Butt, H. J.; Ikeda, T. Supramolecular organogel based on crown ether and secondary ammoniumion functionalized glycidyl triazole polymers. *Macromolecules* **2013**, *46*, 4617-4625.

(2) Wolfe, A. L.; Duncan, K. K.; Lajiness, J. P.; Zhu, K.; Duerfeldt, A. S.; Boger, D. L. A fundamental relationship between hydrophobic properties and biological activity for the duocarmycin class of DNA-alkylating antitumor drugs: hydrophobic-binding-driven bonding. *J. Med. Chem.* **2013**, *56*, 6845-6857.

(3) Gale, J. D.; Rohl, A. L. The general utility lattice program (GULP). *Mol. Simul.* **2003**, *29*, 291-341.

(4) EXSYCalc, Mestrelab Research S.L., accessed Oct. 24, **2017**.